NASA TECHNICAL MEMORANDUM

NASA TM X- 67853

NASA TM X- 67853

COMPARISON OF TWO AND THREE DIMENSIONAL STEADY-STATE THERMAL ANALYSES OF A HEAT SOURCE CONSIDERED FOR ISOTOPE BRAYTON

by Raymond K. Burns
Lewis Research Center
Cleveland, Ohio

May, 1971

This information is being published in preliminary form in order to expedite its early release.

COMPARISON OF TWO AND THREE DIMENSIONAL STEADY-STATE THERMAL ANALYSES OF A HEAT SOURCE CONSIDERED FOR ISOTOPE BRAYTON

by

Raymond K. Burns

Lewis Research Center

SUMMARY

Two and three dimensional thermal analyses have been performed to predict the internal temperatures in an isotope heat source during steady-state operation with a Brayton power system. The heat source design considered is a slight modification of the Pioneer heat source and is referred to herein as IBHS. Two and three dimensional results are compared for a limited range of fuel loadings about the nominal 400 W value and for a range of capsule lengths. Three types of reentry protection insulation sleeves were considered, namely the nickel-zirconia thermal switch, Carb-I-Tex graphite, and two layers of pyrolytic graphite.

Several two dimensional methods to thermally analyzing an IBHS were examined. Two slightly different thermal models were employed. For each of these models two approaches to applying the results to the IBHS were used. One approach consisted of estimating the effective fuel power density (independent of three dimensional results) which was then input to the two dimensional models. This resulted in slightly conservative (high) predictions of IBHS hot-spot temperatures compared to three dimensional results. The other approach consisted of using a small number of three dimensional solutions to develop expressions for effective fuel power density as a function of heat source length and then applying these to the two dimensional thermal models. Such an approach could be used, when many solutions are required, to reduce the time which would be involved if a three dimensional analysis were used to obtain all required solutions.

E-6358

INTRODUCTION

References 1-3 were concerned with the steady-state operational thermal analysis of an isotope heat source which was considered as an energy source for a Brayton system for generation of auxiliary power in space (see refs. 4-5). In the energy source design, a planar array of heat sources radiates thermal energy to the heat source heat exchanger (HSHX). The Brayton cycle working gas is heated to the turbine inlet temperature as

it flows through this heat exchanger. The array of heat sources and its support structure is referred to as the heat source unit (HSU). Each individual heat source, herein called an isotope Brayton heat source (IBHS), consists of a metallic capsule containing Pu^{238} radioisotope fuel and surrounded by graphitic reentry protection materials.

The thermal analyses in references 1-3 were concerned with simulating one IBHS located in the array. In references 2 and 3, a two dimensional thermal model of the IBHS was employed. Since the IBHS is actually a three dimensional entity, assumptions were made concerning the three dimensional heat transfer effects in applying the two dimensional model. Full evaluation of these assumptions could be made with a three dimensional analysis, but this had not been done at that time. In reference 1, a three dimensional thermal model was employed, but it was simplified by neglecting some of the heat transfer paths in the end regions of the heat source. Because of these simplifications this thermal model was known to be conservative.

The purpose of this report is to present some results of a complete three dimensional analysis of an IBHS during steady-state power system operation and to compare these results to two dimensional predictions. Two dimensional results are dependent on the assumptions which are necessary to apply them to an actual IBHS. Several methods of applying two dimensional analyses are considered here, including the one used in reference 2. The results are given over a range of fuel loadings of ± 10 percent about the nominal 400 W and over a range of fuel capsule length from the 6.3-inch length considered for the IBHS to the 4.8-inch length of the fuel capsule in the heat source for the Pioneer mission isotope thermoelectric generator.

DESCRIPTION OF THE HEAT SOURCE AND THE HEAT SOURCE UNIT

The isotope Brayton heat source (IBHS) considered for analysis here and in references 1-3 is shown in figure 1. It is a derivative of the heat source being developed by the AEC for the Pioneer mission isotope thermoelectric generator. The fuel is contained within a hemispherically capped, cylindrical, refractory metal capsule. The structural member is T-111 (a tantalum alloy) and is separated from the fuel by a tantalum -10 percent tungsten liner. The T-111 is covered by a platinum -20 percent rhodium oxidation resistance clad. The fuel is distributed throughout the cylindrical portion of the capsule. The hemispherical end regions are filled by foamed molybdenum spacers.

The fuel capsule is vented, and a pressure retention device is included in one end (not shown in figure 1) to maintain

a helium pressure of 1.0 to 6.0 psia within the platinum -20 percent rhodium clad. In the thermal analysis, it is assumed that all gaps within the capsule are helium filled.

A heat source consists of a fueled capsule and its reentry protection. The IBHS reentry protection considered in this analysis consists of POCO and Carb-I-Tex graphites and insulation materials. The cylindrical portion of the capsule is surrounded by a sleeve of reentry insulation. This is then surrounded by an outer sleeve of POCO graphite which has a hexagonal exterior shape. Two threaded Carb-I-Tex end plugs hold the capsule within the POCO sleeve. In the IBHS configuration considered here, the end plugs are separated from the capsule by 6 percent dense tantalum felt compliance pads. A layer of TZM (molybdenum alloy) is included between the compliance pads and the end plugs.

Several types of reentry insulation sleeves are considered for the IBHS. Thermal results for heat sources with three types of insulation are given here. One consists of a sleeve of two layers of pyrolytic graphite (PG) with a total thickness of 134 mils. Because of the present uncertainty in the correct value of PG emissivity, all results for this type of insulation are given for two values of emissivity, 0.5 and 0.8. The other insulations considered are a 200-mil-thick sleeve of Carb-I-Tex graphite and a 200-mil-thick sleeve of nickel-zirconia thermal switch material. The thermal switch is a zirconia foam impregnated with nickel. It exhibits an irreversible decrease in thermal conductivity if the material reaches or exceeds the nickel melting temperature ($\sim$2600° F) during atmospheric reentry (see ref. 6). The low thermal conductivity required for thermal protection during reentry does not therefore have to exist during power system operation.

The thermal analysis assumes that for operation with the Brayton system, the heat sources are arranged in a close-packed, circular, planar array (see fig. 2). The IBHS array and its support structure are referred to as the heat source unit (HSU). The thermal energy generated in the fuel is radiated from one side of this planar array to the heat source heat exchanger which is located parallel to it. The thermal analysis presented here and in references 1-3 are intended to simulate a typical IBHS located within the HSU array.

THREE DIMENSIONAL ANALYSIS

Thermal model - The IBHS was thermally simulated by the nodal model shown in figure 3. The model represents one quarter of an IBHS located in a close-packed array. It assumes

that the temperature distribution of a heat source is symmetrical about the two cross-sectional planes bounding the nodal model. The thermal energy generated in the fuel is transferred within the IBHS to the top POCO surfaces where it is then radiated to the HSHX. The total radiation view factors from the POCO surface to the HSHX account for the presence of adjacent heat sources and for reflection and re-radiation of energy between them and the HSHX. Heat transfer to the support structure and to the adjacent heat sources would be small and is neglected. With these thermal boundary conditions, the temperature of each node during power system steady-state operation was determined by use of the CINDA-3G computer code (ref. 7).

The thermal properties of the nodes designated as re-entry insulation were taken as either nickel-zirconia thermal switch, Carb-I-Tex, or pyrolytic graphite (PG) depending on which was being considered for the IBHS. The thermal switch and Carb-I-Tex insulations were assumed to consist of single layers 200 mils thick radially. The PG insulation was taken as two layers, each 67 mils thick, separated by a radiation gap.

The foamed molybdenum end region filler is assumed to have a thermal conductivity equal to that of the fuel and is assumed to be separated from the fuel and the liner by a uniform 10-mil helium-filled gap. The pressure relief device is not included in the model. Helium-filled gaps of uniform 10-mil thickness are assumed to separate the fuel and liner, the liner and structural member, and the structural member and clad. The reentry insulation sleeve is assumed to be separated from the clad and from the POCO graphite by radiation gaps. The tantalum felt compliance pad is assumed to have a thermal conductivity of 0.167 Btu/hr-ft-^{o}F and is assumed to be in contact with the clad and the TZM end cap with negligible thermal contact resistance. The TZM cap is separated from the Carb-I-Tex end plug by either a radiation gap or an assumed thermal conductance. The Carb-I-Tex end plug and the POCO graphite are assumed to be in contact with an assumed value of thermal conductance.

Three Dimensional Results

The key hot spot temperatures in the IBHS with various types of reentry insulation sleeves are given in figures 4-6 as a function of fuel load. The dimensions of the IBHS are those given in figure 1. A variation of 40 watts about the nominal 400-watt fuel load is considered. The sink temperature (HSHX surface temperature) is taken as a uniform 1670^{o} F. In addition to the assumptions already mentioned in the previous section, the contact conductance between the POCO graphite and the Carb-I-Tex end plug was taken as 100 Btu/hr-ft^{2}-^{o}F, and it was assumed that there is a radiation gap between the TZM

and the end plug. The effects of these assumptions are examined later.

For a 400 W fuel load the liner hot spot temperature shown in figure 4 for a thermal switch reentry insulation sleeve is 2200° F and in figure 5 for a Carb-I-Tex reentry insulation sleeve is 2150° F. In the case of PG reentry insulation, two sets of results are given in figure 6a and 6b for two possible values of PG emissivity. For a PG emissivity of 0.8, the liner hot spot temperature is shown as 2200° F and for a PG emissivity of 0.5, it is ~2300° F. For the present HSU geometry and with the assumption that the IBHS temperatures are symmetrical about the central cross sections bounding the thermal model, these hot spot temperatures occur in the longitudinal central cross section at the bottom of the heat source.

The distribution of heat transfer within the IBHS for a 400 W fuel load, for the case shown in figure 4 (thermal switch insulation sleeve) is given in figure 7. Of the total thermal energy generated in the fuel, 90 percent is transferred directly to the cylindrical portion of the liner. The remaining 10 percent is transferred through the foamed molybdenum filler in the end regions and then to the liner. Eighty-one percent of the energy is transferred through the reentry insulation sleeve to the POCO graphite. The remaining 19 percent is transferred through the compliance pad and Carb-I-Tex end plug to the POCO. It can be seen that about half of the energy which is transferred through the compliance pad is transferred from the fuel to the capsule end region longitudinally through the capsule metallic members.

As a result of the relatively high thermal conductivity of the POCO, the distribution of heat transfer from the POCO to the HSHX is rather uniform. The 58 percent shown being transferred from the POCO which surrounds the cylindrical portion of the capsule is from about 52 percent of the area. This is illustrated more clearly in figure 8 where the distribution of radiation transfer per unit heat source length along the length is shown. The flux is normalized with respect to the average flux defined as the total fuel load divided by the total heat source length.

The hot spot temperatures would change with a change in the percent of the energy transferred through the end region. In order to determine the importance of the heat transfer path through the foamed molybdenum filler, a solution was obtained for the same case as shown in figure 7 with the exception that the thermal connection between the filler and liner was removed (equivalent to assuming that the filler is perfectly insulated from the liner). The distribution of heat transfer for this case is shown in figure 9. Although no heat

is transferred from the filler to the liner, 18 percent of the energy generated in the fuel is transferred to the compliance pads around the capsule ends, compared to 19 percent shown in figure 7. This resulted in a liner hot spot temperature prediction of only 5^{o} higher than in figure 4. The heat transfer through the end region filler reduces the longitudinal heat transfer, and hence temperature gradient, in the metallic members, but it does not appreciably change the percentage of heat transferred through the reentry insulation sleeve and does not appreciably change the hot spot temperatures.

The effects of changes in heat transfer through the IBHS end region on the liner hot spot temperature is further illustrated by figure 10. The curve labeled A corresponds to the assumed thermal interfaces used for the results shown in figures 4-6. The curve labeled D is the limiting case in which no heat is transferred through the capsule end, the compliance pads, and the end plugs. The thermal energy is confined to transfer from the fuel, through the reentry insulation sleeve, to the POCO. The heat transfer in the POCO is longitudinal, as well as circumferential and radial, to the top surface from which it is radiated to the HSHX. At 400 W fuel load this case yields a liner hot spot temperature about 70^{o} F higher than case A. This case D is the modified three dimensional model which was employed in reference 1.

The distribution of energy transferred through the reentry insulation sleeve and the end regions also is a function of the capsule length. If the IBHS end region dimensions are held constant and the overall heat source length is decreased by shortening the capsule cylindrical section, the percent of energy transferred through the end regions increases (i.e., the three dimensional heat transfer effects become more significant). A solution was obtained for the case shown in figure 7 except the capsule overall length was reduced to 4.8 inches (the length of the Pioneer mission fuel capsule). This solution predicted that the percent heat transferred through the end regions would be 27 rather than the 19 shown in figure 7 for the 6.3-inch capsule length.

Further three dimensional results are given in a later section when they are compared to the results of two dimensional analyses which are described in the following section.

TWO DIMENSIONAL ANALYSIS

Thermal model - The two dimensional nodal model shown in figure 11 is the same as a cross section of the three dimensional model. It assumes that the temperature distribution is symmetrical about the axial cross section. As in the three dimensional analysis, thermal energy generated in the fuel is transferred from the heat source, only from the top POCO surface, by radiation to the HSHX. However, in the two dimensional analysis, the longitudinal heat transfer in the heat source is not calculated. As in the three dimensional analysis, the nodes denoted as reentry insulation are changed to simulate the nickel-zirconia thermal switch, Carb-I-Tex, or separate layers of pyrolytic graphite.

The intent of the two dimensional model is to predict the IBHS hot spot temperatures during steady-state power system operation. Since the actual IBHS is three dimensional, an effective fuel power density must be used to make the two dimensional model simulate the IBHS. The effective fuel power density can be defined as the fuel load divided by the effective volume of the fuel. The effective fuel volume is a function of three dimensional heat transfer effects in addition to the actual dimensions of the fuel cavity in the capsule.

An obvious way of determining the correct effective fuel power density is by performing a three dimensional analysis for at least one case. When many solutions are required an adjusted two dimensional rather than the three dimensional model can then be employed, with considerable savings in computational time and effort. This approach will be investigated in a later section.

In the absence of a three dimensional analysis some rational approach must be taken to estimate the effective fuel power density as a function of IBHS dimensions and fuel load. Two such approaches will be examined here.

The approach taken in reference 2 to estimate the effective power density was to take the effective fuel volume as the volume of the total fuel cavity, including the hemispherical end regions which are actually filled with foamed molybdenum. Including the end regions is an attempt to account in some way for the longitudinal heat transfer. The effective fuel power density calculated in this way is then used in the two dimensional thermal model where every node is assumed to have a unit depth in the longitudinal direction. This approach will be examined here and will be referred to as method A. The two dimensional model with all nodes at uniform depth will be referred to as two dimensional model I.

Another method to estimate the effective fuel power density is suggested by the fact that the POCO thermal conductivity is relatively high and the capsule is surrounded by relatively low thermal conductivity tantalum felt pads on the ends. The main heat transfer path from the fuel to the POCO is then through the reentry insulation sleeve which surrounds the cylindrical portion of the capsule. This is confirmed by the three dimensional results already presented. The heat is transferred longitudinally, as well as radially and circumferentially through the POCO to the top surface from which it is then radiated to the HSHX. To simulate this, the effective fuel volume could be taken as that of the cylindrical portion of the fuel cavity (which it actually occupies). The depth of the POCO nodes in the two dimensional nodal model could be modified to account for the longitudinal heat transfer in the POCO. This approach is also investigated and is referred to as method B. The two dimensional model employed in this method, which includes POCO nodes of modified depth, is referred to as two dimensional model II.

In two dimensional model II, the POCO nodes have been made deeper in the longitudinal direction than all others by the ratio of the total IBHS length to the length of the cylindrical section of the capsule (the fueled length). This amounts to assuming that the total heat generated in the fuel is transferred uniformly from the IBHS POCO surface along its entire length. The three dimensional results previously presented showed this to be a reasonable approximation (see figure 8).

Two Dimensional Results

The cross sectional dimensions of the two dimensional nodal models shown in figure 11 are those of the IBHS as shown in figure 1. For these cross sectional dimensions, two dimensional thermal results can be generated as a function of effective fuel power density. When the two dimensional model II is used, the ratio by which the POCO nodes are deepened must also be specified.

In figures 12 through 17, the key hot spot temperatures are plotted as a function of the effective fuel power density, with each figure considering an IBHS with a different reentry insulation sleeve. The results given in these figures can be related to the IBHS as a function of fuel load and capsule length by use of one of the methods for estimating the effective fuel power density. The curves in figures 12-14 were obtained using the two dimensional thermal model I and are for use in method A and the curves in figures 15-17 were obtained using thermal model II and are for method B. The effective fuel volume and the effective fuel power density for a 400 W

fuel load are given in figure 18 for method A and B.

In the next section figure 18 will be used, together with the results in figures 12-17 to compare methods A and B. These two dimensional results will also be compared to three dimensional results. Finally, the three dimensional results will be used to determine an effective fuel power density independent of figure 18 which can then be applied to both sets of results in figures 12-17. These will be referred to as methods C and D.

COMPARISON OF TWO AND THREE DIMENSIONAL ANALYSES

Methods A and B - The hot spot temperatures predicted by use of two methods (previously designated A and B) of applying the two dimensional thermal models to the IBHS are compared in figures 19-22 to results obtained from a three dimensional analysis. In figures 19-21 the temperatures are plotted as a function of fuel load for a 6.3-inch long capsule and for three types of reentry insulation sleeve. It can be seen that both two dimensional methods are conservative (high) in predicting the fuel, liner and T-111 hot spot temperature for these cases. Method B predicts a POCO hot spot temperature very close to that of the three dimensional analysis, while method A is conservative.

The steady-state operating temperature of prime interest for the IBHS of this analysis is the liner hot spot temperature. The predictions of this temperature made by methods A and B for the thermal switch and Carb-I-Tex insulation cases in figures 19 and 20 are comparable. For a 400 W fuel load, they are 50-60^{o} F higher than the three dimensional predictions for the thermal switch case and 35-40^{o} F higher than the three dimensional results for the Carb-I-Tex case. For the IBHS with two layers of PG reentry insulation considered in figure 21, method B is clearly more conservative than method A.

In figure 22, an IBHS with thermal switch insulation and 400 W fuel load is considered as a function of capsule length. For these results the IBHS end region dimensions were held fixed and the capsule cylindrical region length was varied. The results are given as a function of capsule overall length which, for reference, is 6.3-inches for the IBHS considered in this analysis and shown in figure 1, and 4.8 inches for the Pioneer mission thermoelectric generator heat source. It can be seen that both methods A and B are conservative (higher than three dimensional predictions) for the range of lengths considered. As the capsule is shortened, the conservatism of method B increases faster than that of method A. As expected, as the length increases (and three dimensional effects

are consequently reduced) the results of both two dimensional methods approach the three dimensional results.

In all the cases considered thus far, both two dimensional methods have been found to be conservative but adequate for engineering calculations. In the absence of a three dimensional calculation for each particular case, it would be desirable to be able to predict whether a two dimensional approach would be conservative or optimistic. It is difficult to determine a priori whether method A is conservative since it is difficult to estimate whether assuming that the fuel is distributed into the capsule ends in calculating the effective fuel power density properly compensates for longitudinal heat transfer. Method B is conservative in that it neglects heat transfer through the end of the capsule and it is optimistic in that it effectively assumes that the longitudinal thermal resistance of the POCO is zero. In a heat source such as the IBHS considered here, the longitudinal resistance to heat transfer in the POCO actually is quite small in comparison to the radial resistances of the insulation and the gaps between elements of the heat source. The three dimensional results presented in a previous section (figure 8) have indicated that the heat transfer from the POCO to the HSHX is fairly uniform along the IBHS length. It is therefore indicated that the optimistic element in method B is small and overall, method B is generally conservative. Method B then has some advantage over method A in that in the absence of a three dimensional analysis the conservatism of method B is rather easily assured while it is difficult to determine whether or not method A is conservative because of the assumptions involved.

Methods C and D - The thermal results given in figures 12-17 as a function of effective fuel power density were obtained using two slightly different thermal models. Those used in method A, figures 12-14, were obtained using a model in which all nodes were of uniform longitudinal depth (two dimensional model I). For method B, the results in figures 15-17 were obtained using a thermal model in which the POCO nodes were deeper in the longitudinal direction than the others (two dimensional model II). Methods A and B consist of applying these results to the IBHS using estimates of the effective fuel volume (or fuel power density) given in figure 18. When a three dimensional thermal model is available, an alternative approach would be to use a small number of three dimensional solutions to determine the effective fuel volume of the heat source. These effective fuel volumes would then be used, instead of those in figure 18, with the results of both two dimensional thermal models I and II to predict the heat source temperatures. Use of the results of two dimensional model I in this way is designated as method C and

use of the results of two dimensional model II is designated as method D. In this way the accuracy of the two dimensional approach could be improved over methods A and B. When many solutions are required, the two dimensional model could then predict the IBHS hot spot temperatures with accuracy approaching the three dimensional analysis, but with much less computing time than use of the three dimensional model would require.

The effective fuel power density of a heat source is defined as the total fuel load divided by the fuel effective volume:

$$Q_E''' = \frac{Q}{V_E} \qquad (1)$$

In addition, it is assumed that the effective fuel volume can be written as the product of a parameter α and some characteristic length of the HS:

$$V_E = \alpha L \qquad (2)$$

Assuming that the factor α is independent of fuel load and heat source length it can be determined from a single three dimensional result for each heat source design. It will later be shown that for method D it is necessary to allow α to vary linearly with length (requiring two three dimensional solutions to determine it) to make the accuracy of method D comparable to that of method C for constant α when heat source length is varied. Once this factor α is determined for a heat source design it can then be used in equations (2) and then (1) to determine the effective fuel power density as a function of heat source fuel load and length. The characteristic length in equation (2) is taken as the overall capsule length for method C and as the length of the cylindrical portion of the capsule (the fueled length) for method D.

To illustrate the determination of the factor α, consider the three dimensional results for the IBHS with thermal switch insulation, 6.3-inch long capsule, and 400 W fuel load given in figure 4. The liner hot spot is calculated to be 2197° F. In figure 12, it can be seen that using an effective fuel power density of 18.8 W/in^3 with two dimensional model I would give the same liner hot spot temperature. Using this power density and equations 1-2 for 400 W fuel load and 6.3-inch length yields a value of 3.38 in^2 for α. This value can then be used to calculate the effective power density for method C for other fuel loads and heat source lengths. Using the two dimensional model II, the results in figure 15 show that an effective power density of 25.3 W/in^3 would yield a liner hot spot temperature of 2197° F. This value in equations 1-2 with a 400 W fuel load and a characteristic length of

3.84 inch (the fueled length for a 6.3-inch overall length capsule) yields a value of 4.12 in^2 for α at this length for method D. The value of α for each method is assumed not to vary with fuel load. It will be shown that it can be assumed to be independent of length for method C and to vary linearly with length for method D. The factor α does vary with changes in IBHS configurations such as changes in the reentry insulation sleeve materials.

Determining the effective fuel power densities in this way, the hot spot predictions of methods C and D are compared to three dimensional results for heat sources with three types of reentry insulation in figures 23-25. In each case, the factor α for each method was determined to make the liner hot spot temperatures predicted by two dimensional models agree with the three dimensional results at a fuel load of 400 W. As shown in figures 23-25, the liner hot spot predictions of both two dimensional methods agree closely with the three dimensional predictions over the range of fuel loadings considered, indicating that the factor α actually is nearly independent of fuel loading in this range.

Although both methods C and D are made to closely agree with the three dimensional results on liner hot spot, they both slightly underestimate the fuel hot spot temperature. Method C predicts a POCO hot spot temperature above the three dimensional results while method D underestimates it. Figures 23-25 show that method D more closely predicts the fuel and T-111 hot spot temperatures than does method C.

In figure 26 the two dimensional methods are compared to three dimensional results as a function of heat source length for an IBHS with thermal switch reentry insulation and 400 W fuel load. For method C, the factor α was determined at a 6.3-inch capsule length. As shown in figure 26b, this results in good agreement with the three dimensional results in predicting the liner hot spot temperatures throughout the range of lengths considered indicating that for method C, the factor α is nearly independent of length. However, for method D, the factor α was found to be more dependent on length. In figure 26b, the method D results shown with a broken line were obtained by using a factor α determined at a capsule length of 6.3 inches. As shown this results in a disagreement with the three dimensional results of over 50° F at a capsule length of 4.8 inches. In order to make method D agree with the three dimensional predictions for liner hot spot temperature as well as method C does in figure 26b, it was necessary to allow α to vary linearly with capsule length. This requires two three dimensional solutions to determine α. In figure 26, the method D results shown by the unbroken lines

were obtained using an α which varied linearly between the values determined from three dimensional results for 4.8 inch and 6.3-inch long capsules. Allowing the α to vary in a similar manner for method C would not result in a material improvement over the results shown in figure 26 for constant α .

CONCLUDING REMARKS

A three dimensional analysis of an IBHS (Isotope Brayton heat source) with 400 W fuel load, located in a close-packed planar array and radiating to a 1670° F sink temperature predicted that:

1. The liner hot spot temperature is about 2200° F if a thermal switch insulation sleeve is used and about 2150° F if a Carb-I-Tex graphite insulation sleeve is used. With an insulation sleeve consisting of two layers of PG (pyrolytic graphite), the liner hot spot is about 2200° F if the PG emissivity is 0.80 and 2300° F if the PG emissivity is 0.50. This illustrates the significant effect of the radiation gaps assumed to exist between the reentry protection materials and the importance of accurately knowing the thermal properties of the materials, including emissivity.

2. The main heat transfer path from the fuel to the POCO graphite is through the reentry insulation sleeve which surrounds the cylindrical part of the capsule. The longitudinal heat transfer in the POCO is sufficient to make the variation in distribution of heat transfer from the POCO to the HSHX(heat source heat exchanger) along the heat source length less than 10 percent from the average. Heat transfer through the foamed molybdenum end region fillers reduces the longitudinal heat transfer in the capsule metallic members from what would occur if no heat were transferred through the filler, but it does not substantially affect the percent of energy transferred to the compliance pad or the liner hot spot temperature.

Several two dimensional methods were examined and compared to the three dimensional results for an IBHS. Two slightly different two dimensional thermal models were used. Model I had all nodes of uniform longitudinal depth. The other, Model II, was a slight modification, with the POCO graphite nodes deeper longitudinally than other nodes. For each of the thermal models, two approaches to applying the results to the IBHS were considered. One approach consisted of estimating the effective fuel power density, independent of three dimensional results, and the other consisted of

using a small number of three dimensional solutions to determine the effective fuel power density.

The two dimensional methods designated A and B use rational estimates for the effective fuel power density. Method A employed two dimensional thermal model I and method B used thermal model II. Both methods A and B were found to be conservative (high) in predicting hot spot temperatures of the IBHS in comparison to three dimensional results, but both methods could be used in engineering calculations. Method B predicts slightly higher temperatures and in the absence of three dimensional results it is easier to predict that it is conservative for any particular case.

Methods C and D consist of using a small number of three dimensional solutions to determine the effective fuel power densities for the two dimensional thermal models I and II respectively. In these methods, one or two three dimensional solutions are used to develop an expression for the effective fuel power density as a function of heat source length and fuel loading for each heat source design. The two dimensional models can then be used in situations where many solutions are required. The hot spot temperatures predicted by both methods were relatively close to the three dimensional predictions for the range of variables considered. Method D resulted in closer agreement with three dimensional results on all hot spot temperatures than did method C.

REFERENCES

1. Burns, Raymond K.: A Parametric Thermal Analysis of an Isotope Brayton Heat Source Design During Steady State Operation. NASA TM X-52948, 1970.

2. Cropp, L. O.: Two-Dimensional Steady-State Operational Thermal Analysis of the Isotope Brayton Heat Source. Rep. SC-RR-70-451, Sandia Lab., Aug. 1970.

3. Burns, Raymond K.: Preliminary Analysis to Determine the Reentry Insulation Requirements on a Pioneer-Type Heat Source for Use in the Isotope Brayton Application. NASA TM X-52850, 1970.

4. Brown, William J.: Brayton-B Power System - A Progress Report. Proceedings of the 4th Intersociety Energy Conversion Engineering Conference. AIChE, 1969, pp. 652-658.

5. Klann, John L.: Steady-State Analysis of a Brayton Space Power System. NASA TN D-5673, 1970.

6. Anon.: High-Temperature Metal Thermal Switch Development Program First Quarterly Report, July-August 1969. Hittman Associates, Inc., Mar. 1970. (Work under Contract AT (29-2)-2797).

7. Lewis, D. R.; Gaski, J. D.; and Thompson, L. R.: Chrysler Improved Numerical Differencing Analyzer for Third Generation Computers. Rep. TN-AP-67-287, Chrysler Corp. (NASA CR-99595), Oct. 20, 1967.

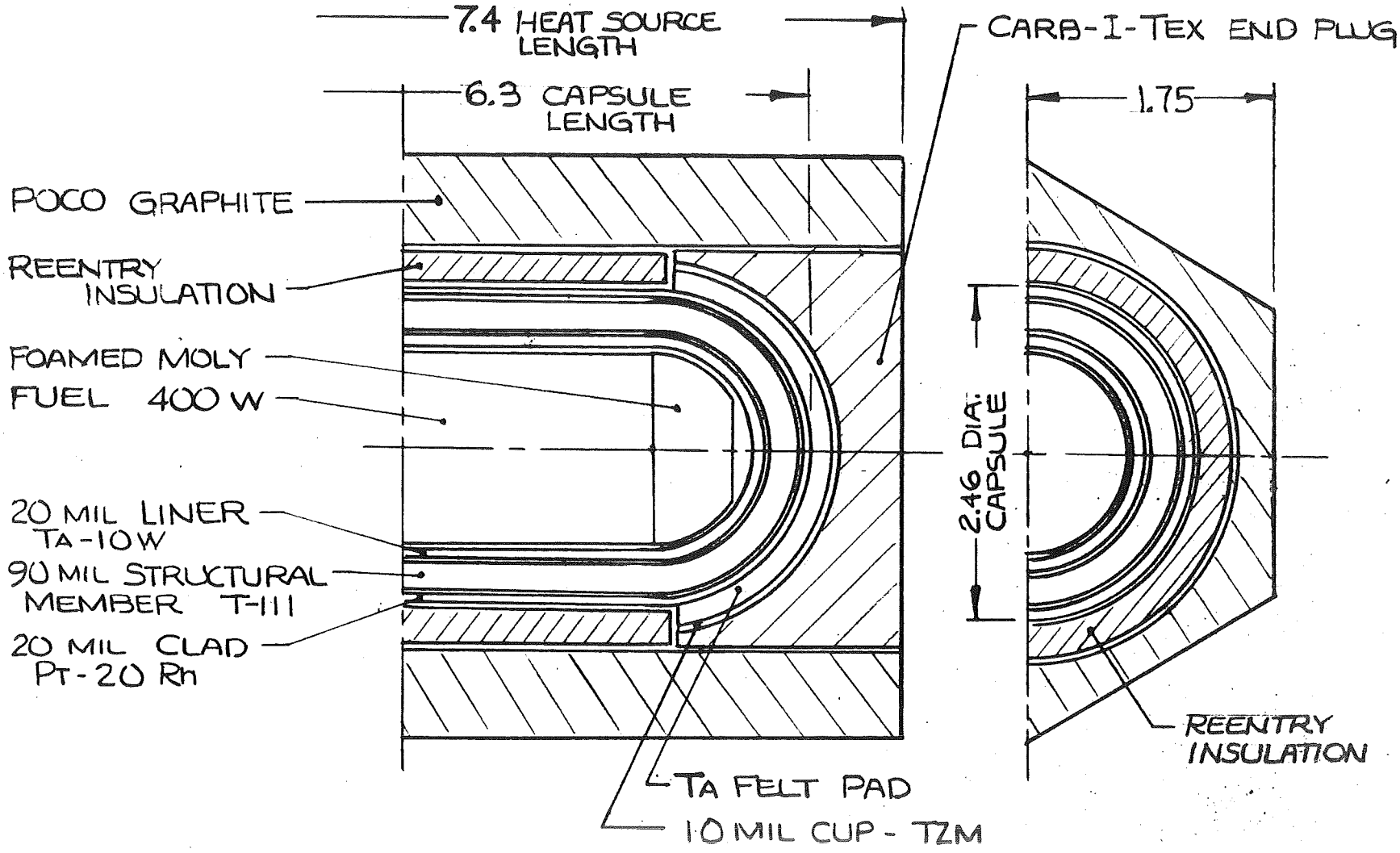

FIGURE 1 SKETCH OF HEAT SOURCE (IBHS)

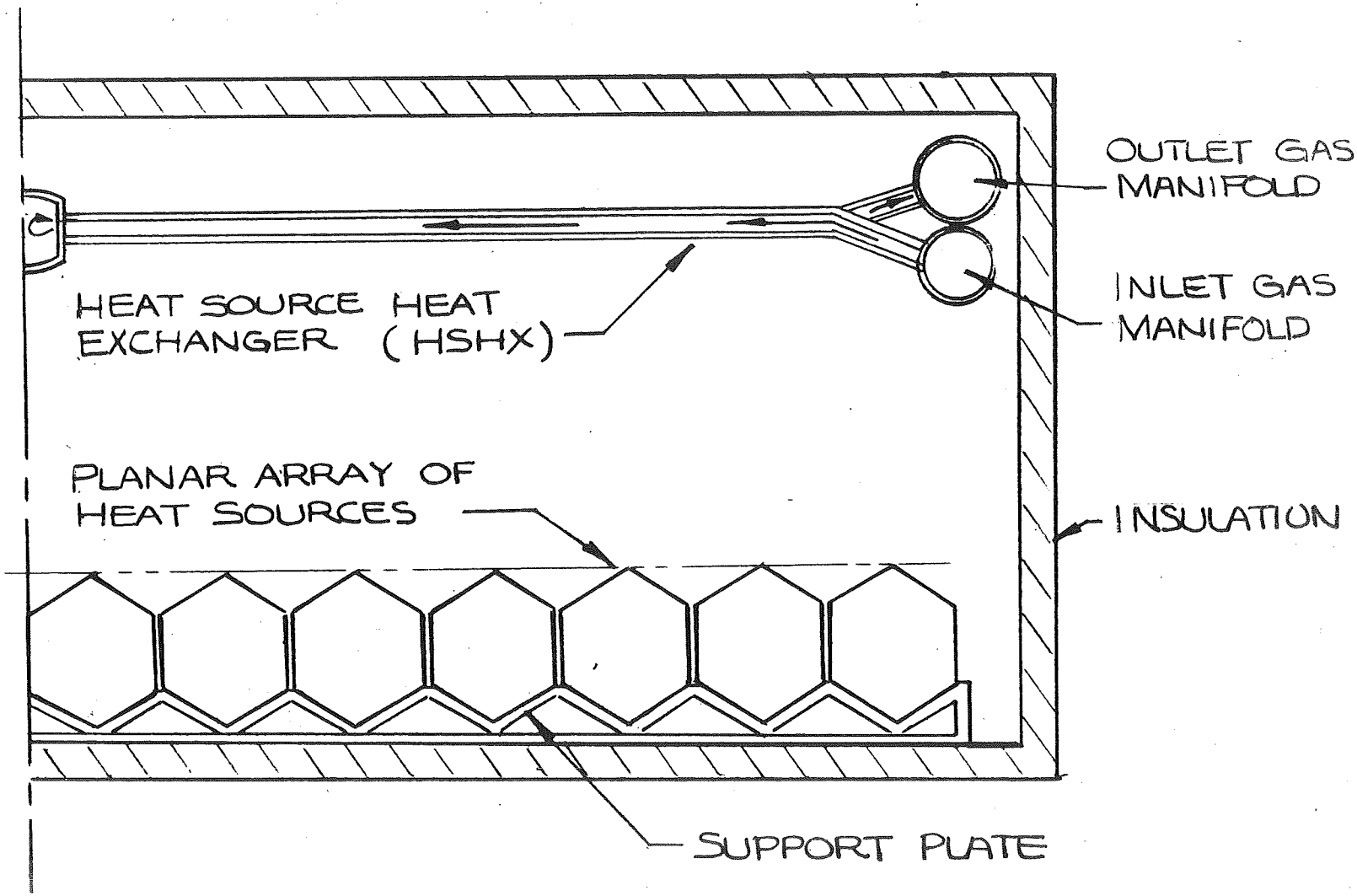

FIGURE 2 SKETCH OF HEAT SOURCE UNIT

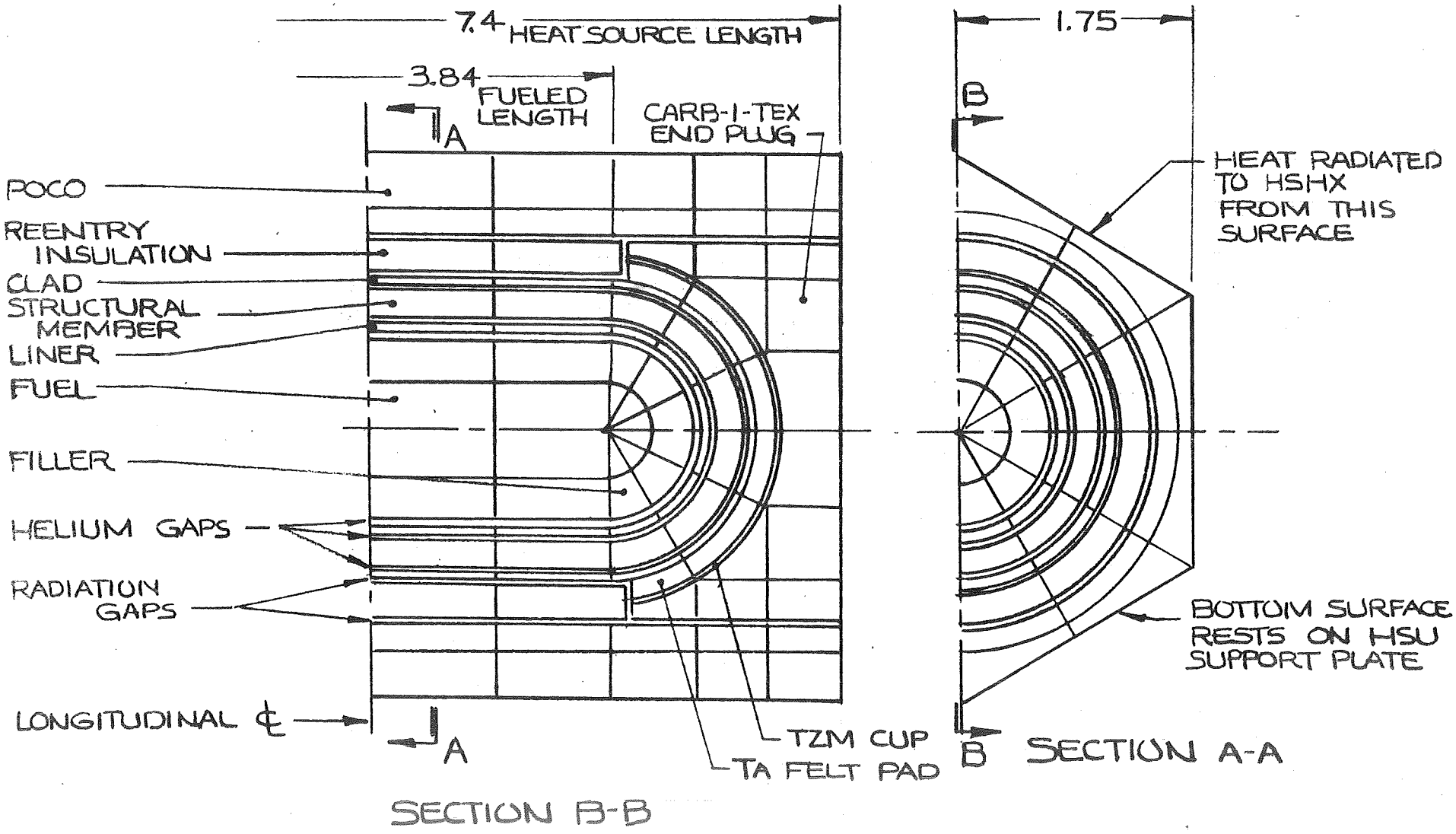

FIGURE 3 THREE DIMENSIONAL THERMAL MODEL OF AN IBHS

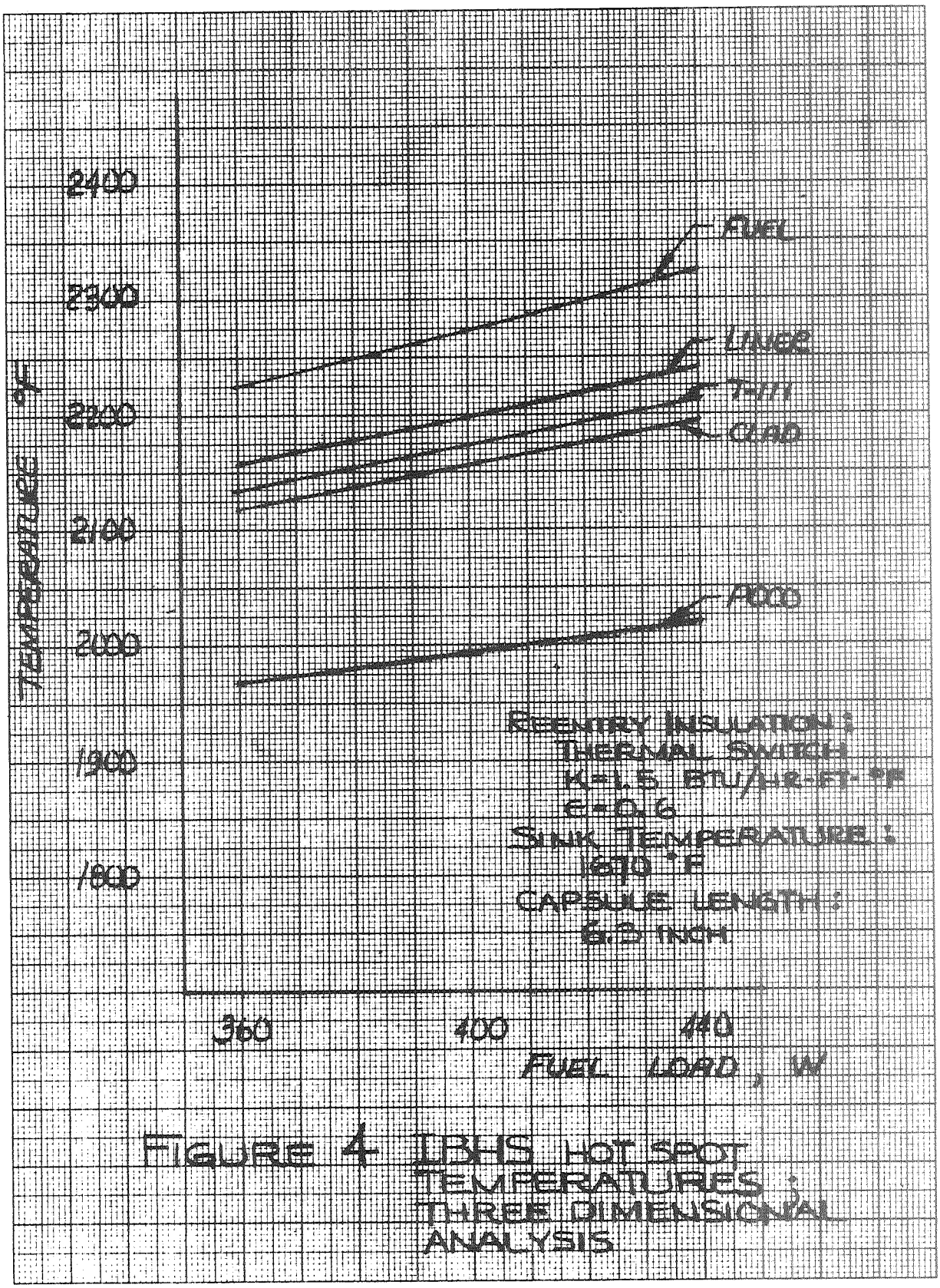

FIGURE 4 IBHS HOT SPOT TEMPERATURES; THREE DIMENSIONAL ANALYSIS

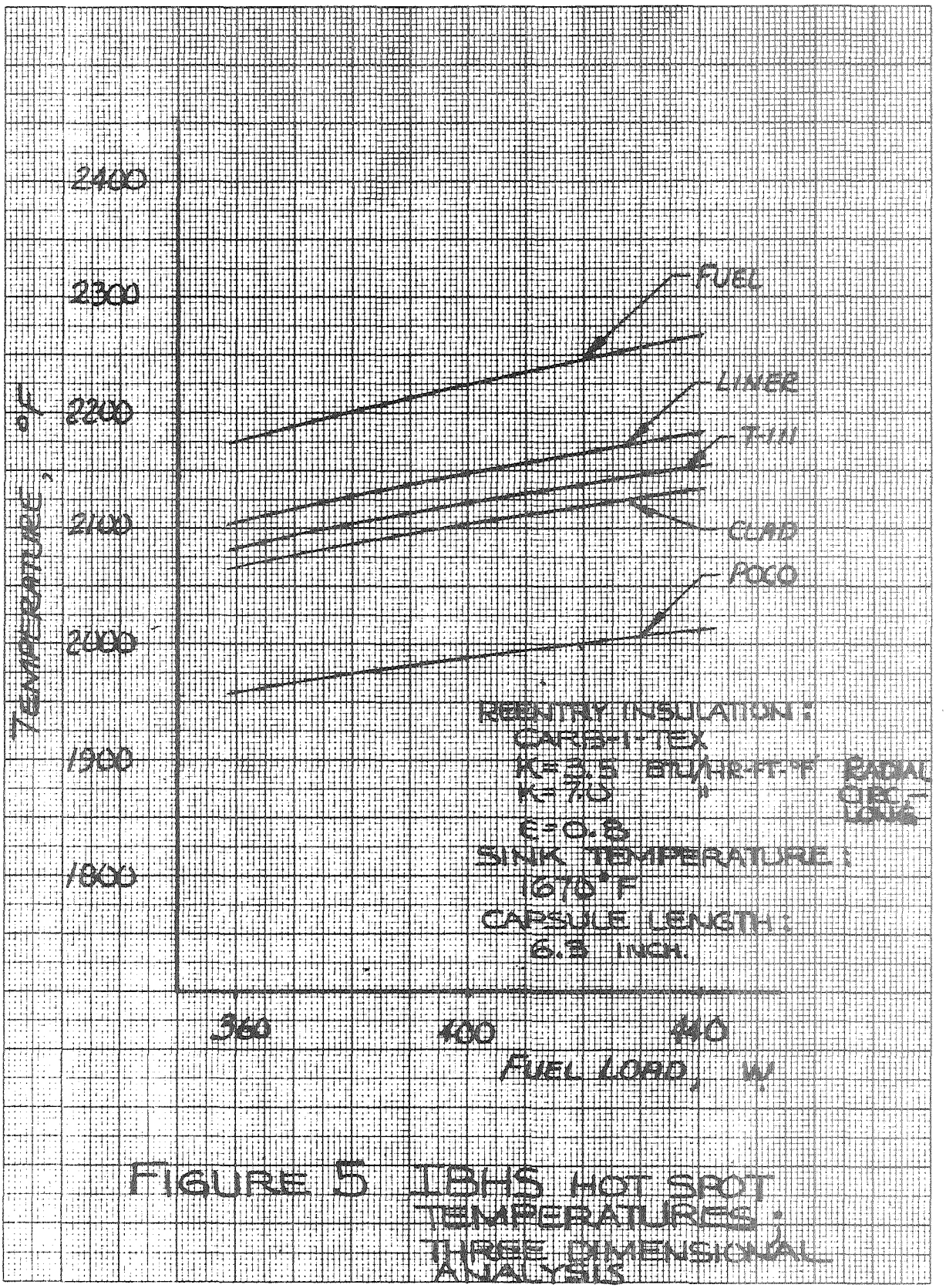

FIGURE 5 IBHS HOT SPOT TEMPERATURES - THREE DIMENSIONAL ANALYSIS

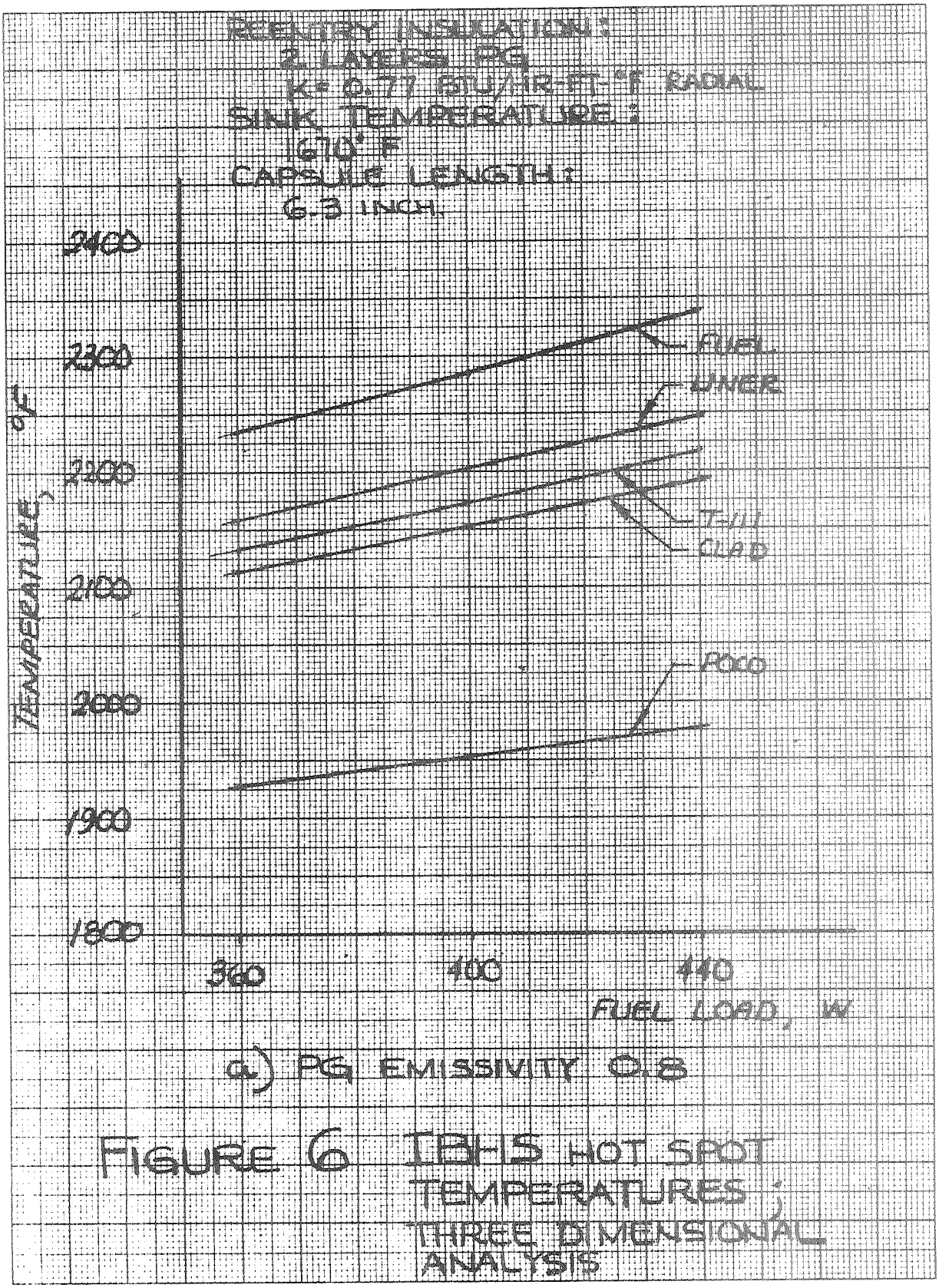

FIGURE 6 TBHS HOT SPOT TEMPERATURES, THREE DIMENSIONAL ANALYSIS

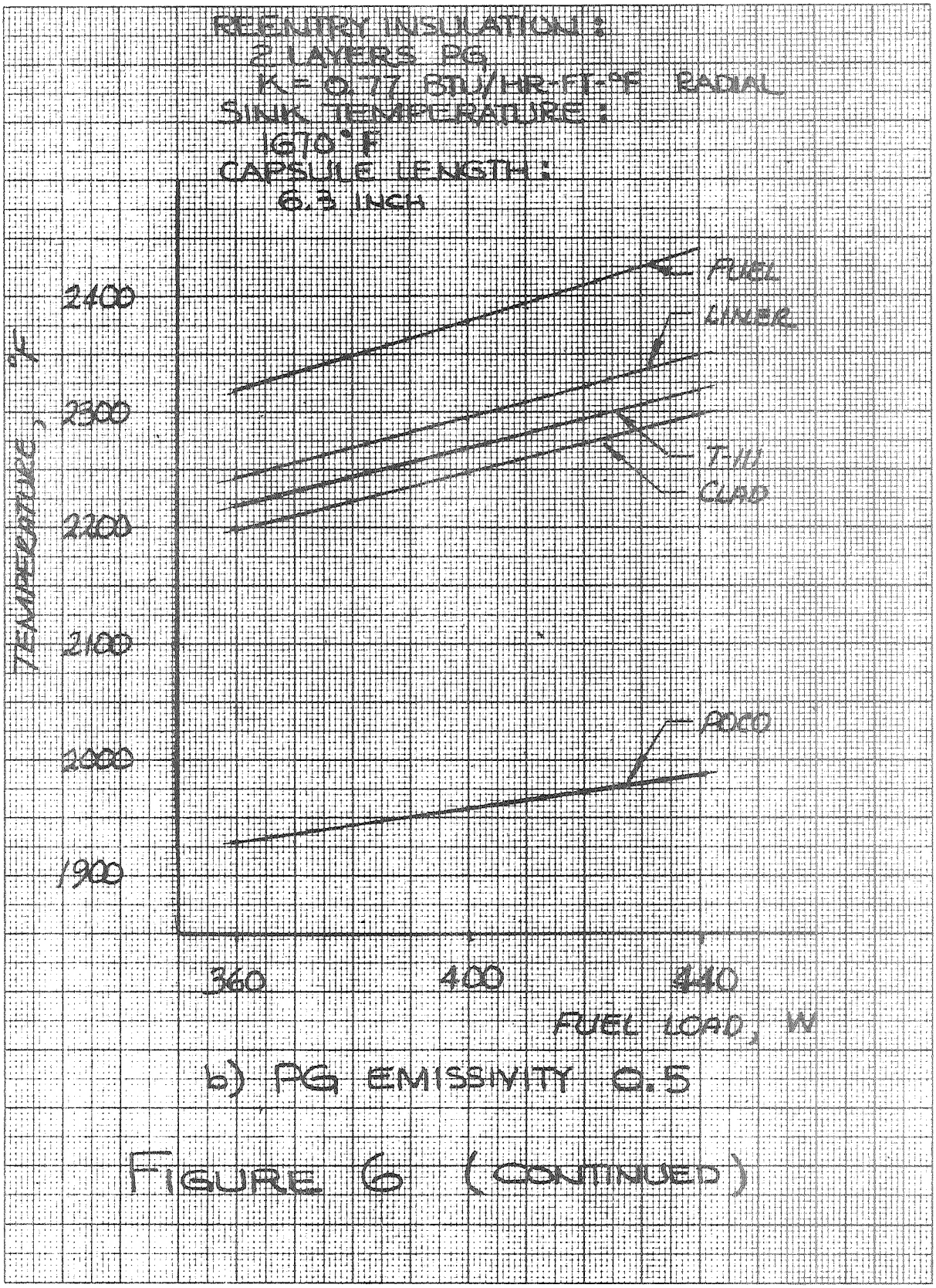

b) PG EMISSIVITY 0.5

FIGURE 6 (CONTINUED)

FIGURE 7 IBHS DISTRIBUTION OF HEAT TRANSFER; 400 W FUEL LOAD, THERMAL SWITCH INSULATION, 6.3 IN. LONG CAPSULE, 1670° F SINK TEMPERATURE

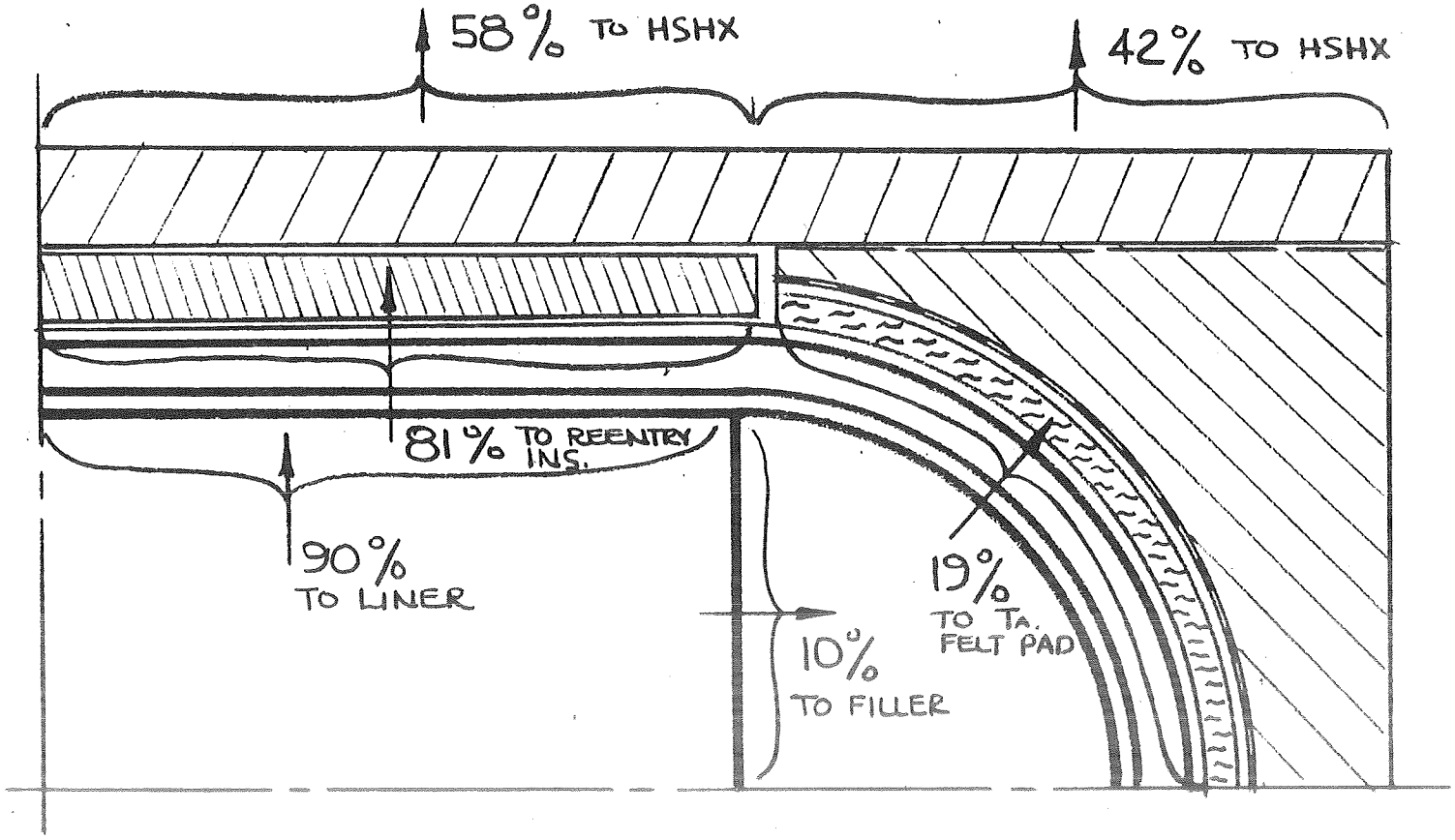

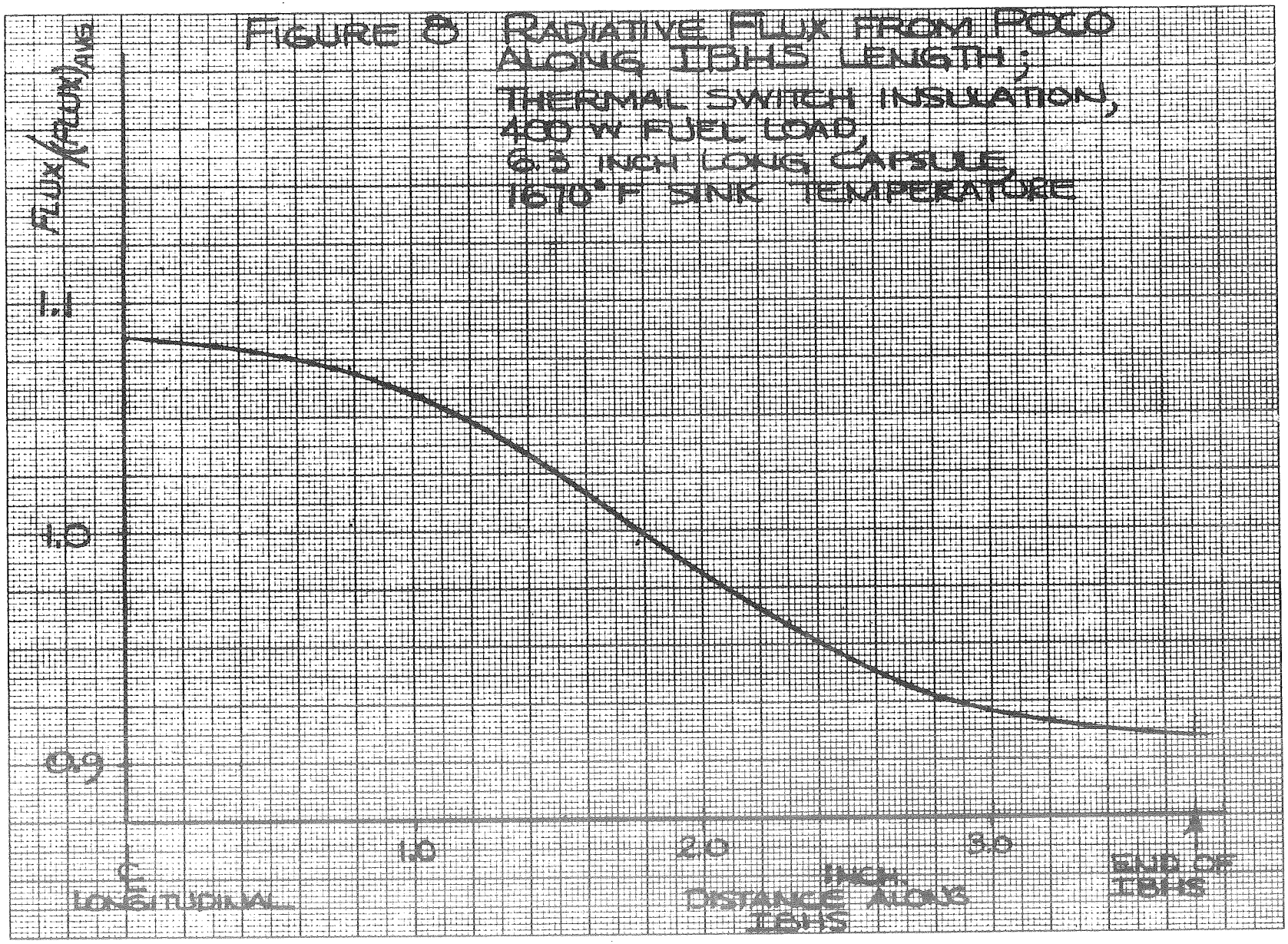
FIGURE 8 RADIATIVE FLUX FROM POCO ALONG IBHS LENGTH; THERMAL SWITCH INSULATION, 400 W FUEL LOAD, 6.3 INCH LONG CAPSULE, 1670°F SINK TEMPERATURE
FLUX/(FLUX)AVG
1.1
1.0
0.9
0
LONGITUDINAL
1.0
2.0
3.0
INCH
DISTANCE ALONG IBHS
END OF IBHS

FIGURE 9 IBHS DISTRIBUTION OF HEAT TRANSFER WITH NO HEAT TRANSFER THROUGH END FILLER ; 400 W FUEL LOAD, THERMAL SWITCH INSULATION, 6.3 IN. LONG CAPSULE, 1670°F SINK TEMPERATURE

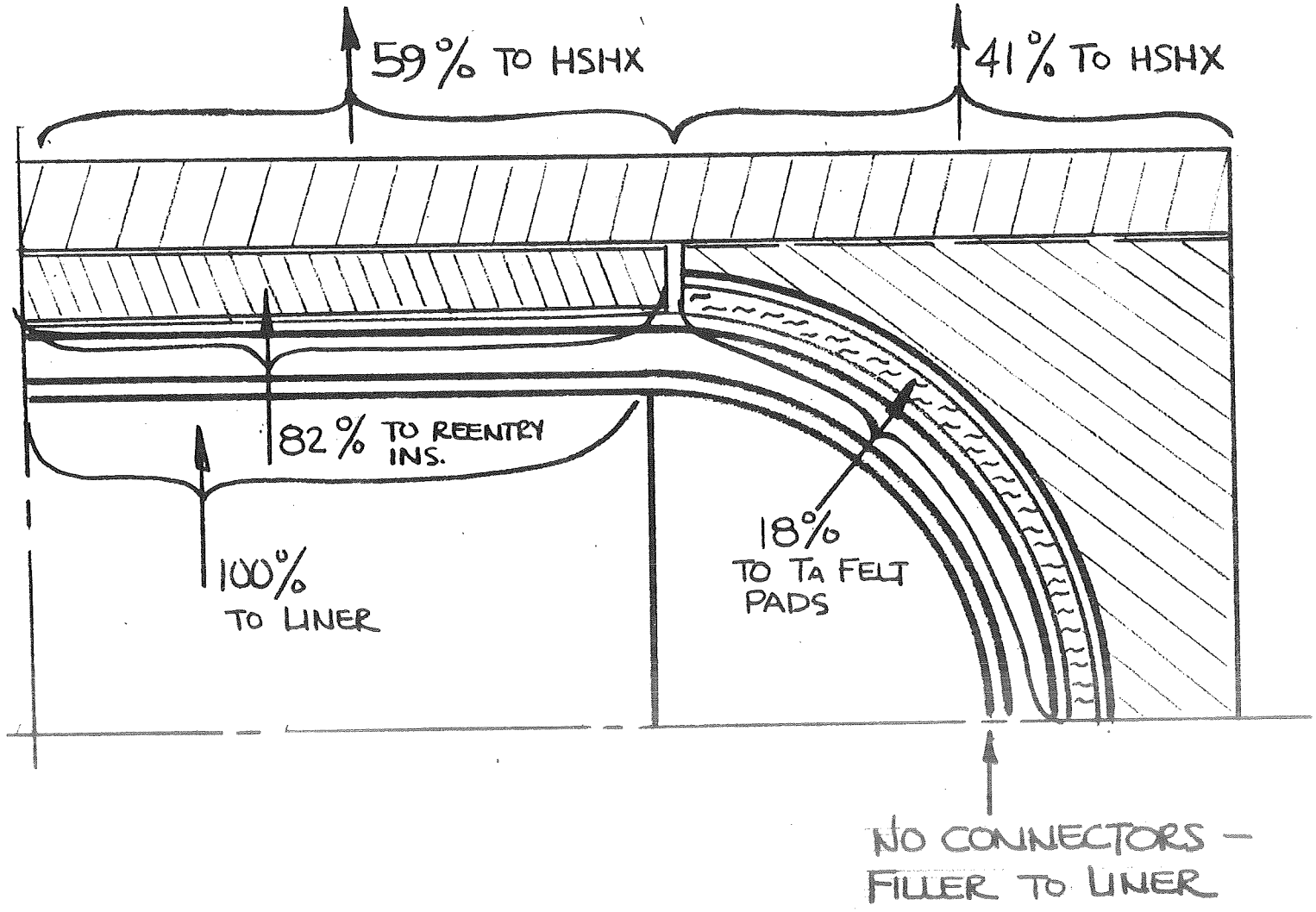

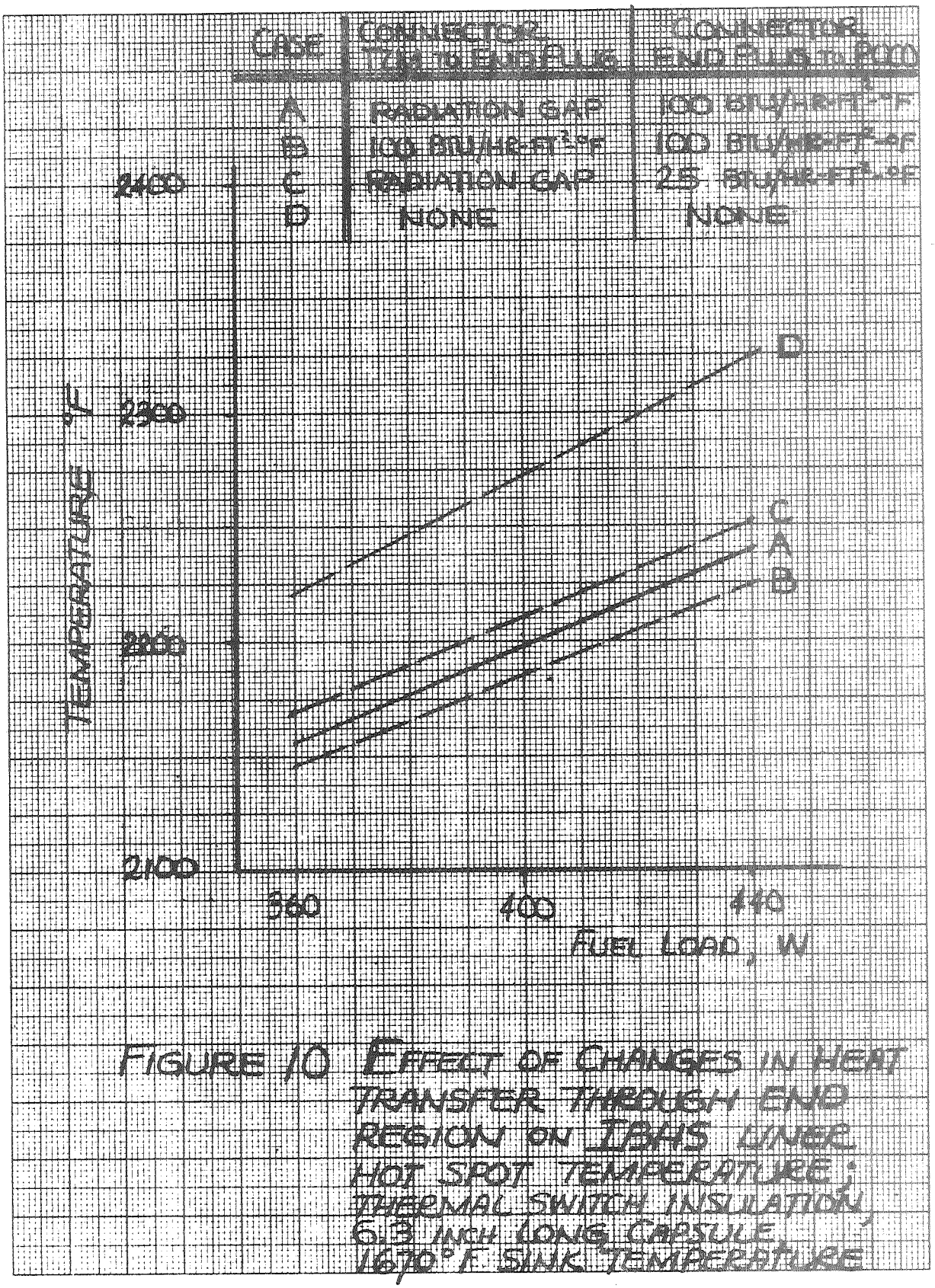

FIGURE 10 EFFECT OF CHANGES IN HEAT TRANSFER THROUGH END REGION ON IBAS LINER HOT SPOT TEMPERATURE; THERMAL SWITCH INSULATION, 6.3 INCH LONG CAPSULE, 1670° F SINK TEMPERATURE

THERMAL MODEL I:
ALL NODES UNIFORM DEPTH

THERMAL MODEL II:
POCO NODES DEEPER THAN OTHERS
BY RATIO OF IBHS LENGTH
TO CAPSULE FUELED LENGTH

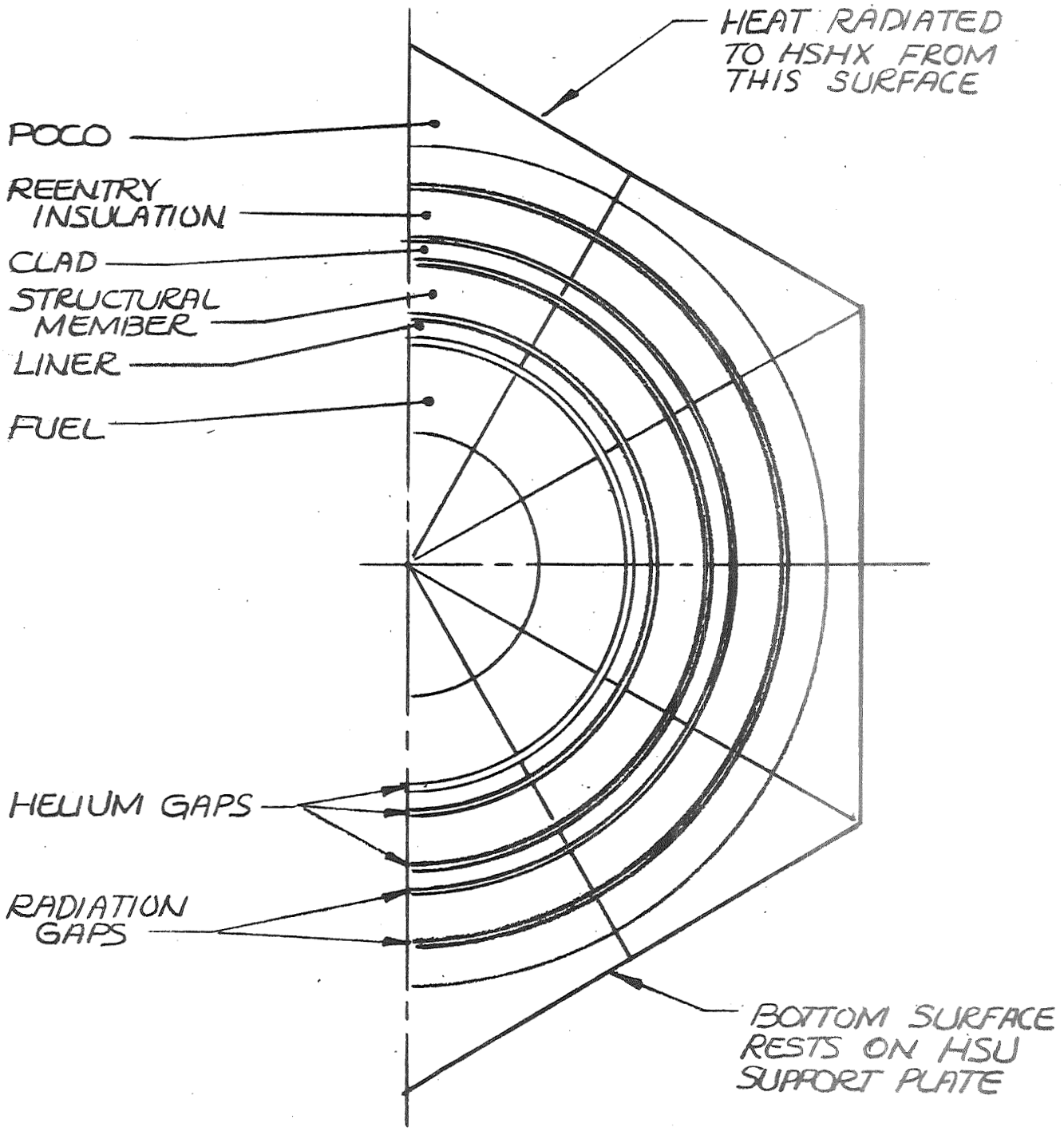

FIGURE 11 TWO DIMENSIONAL THERMAL MODEL OF IBHS

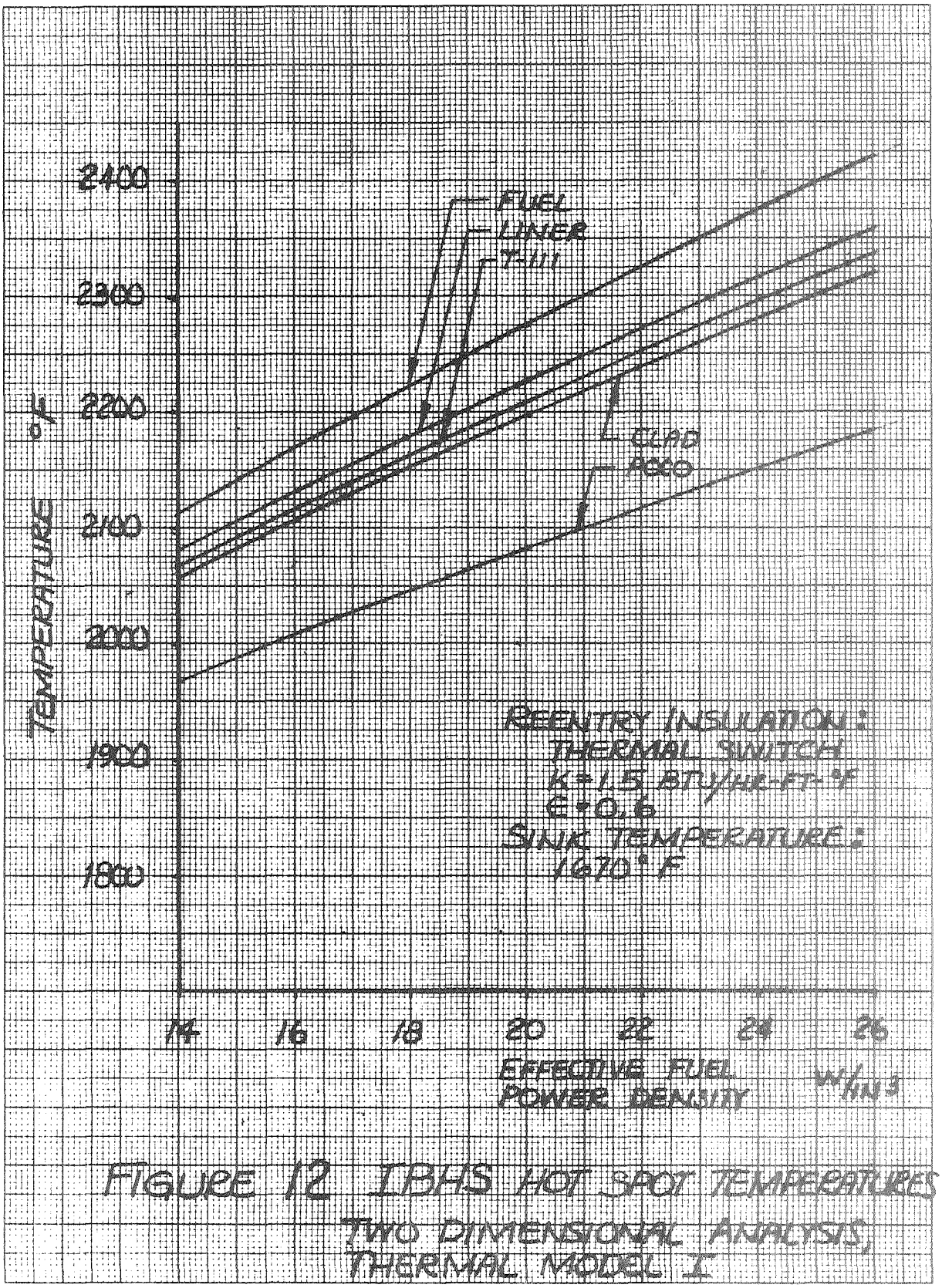

FIGURE 12 IBHS HOT SPOT TEMPERATURES
TWO DIMENSIONAL ANALYSIS
THERMAL MODEL I

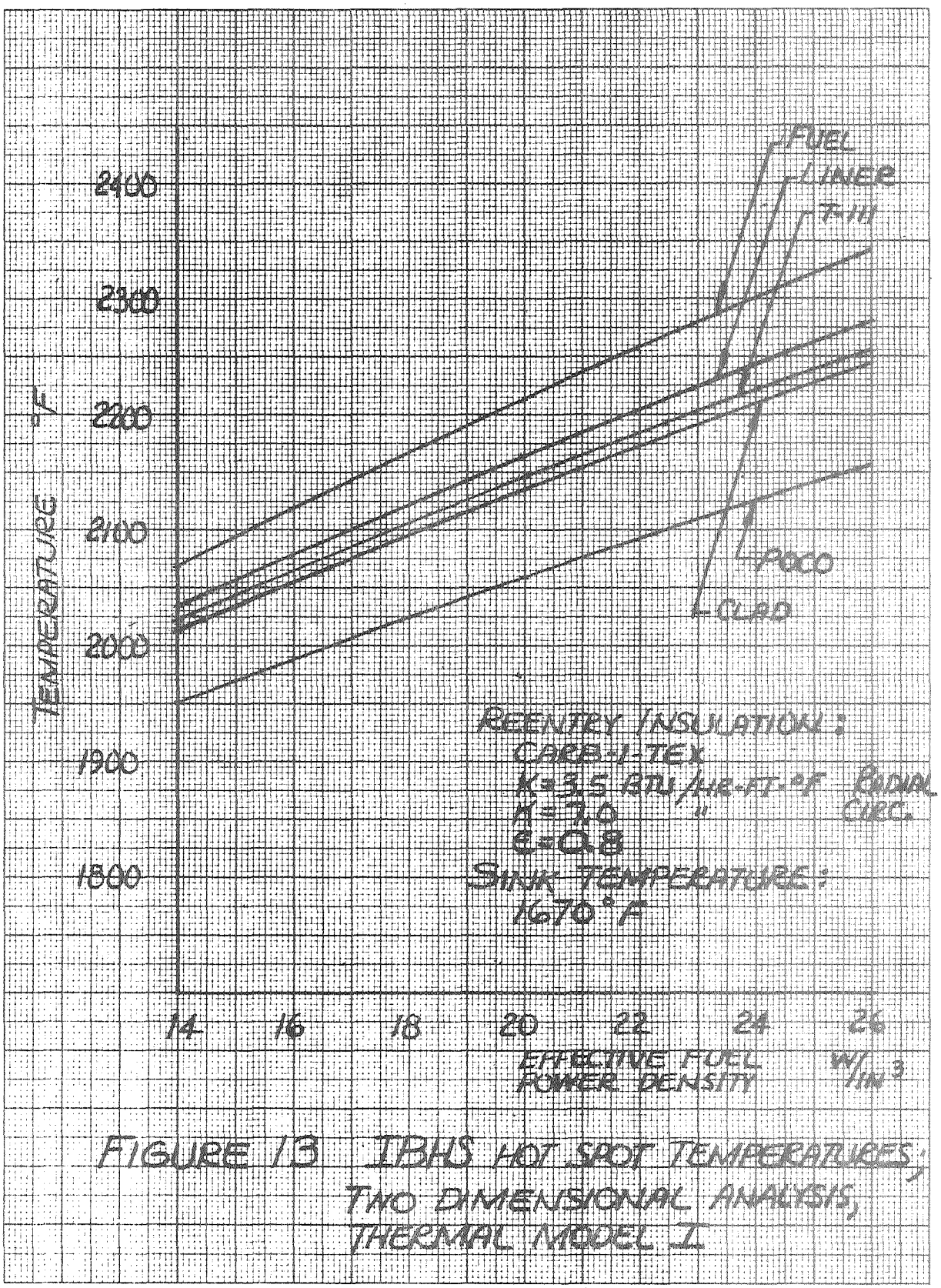

FIGURE 13 IBHS HOT SPOT TEMPERATURES, TWO DIMENSIONAL ANALYSIS, THERMAL MODEL I

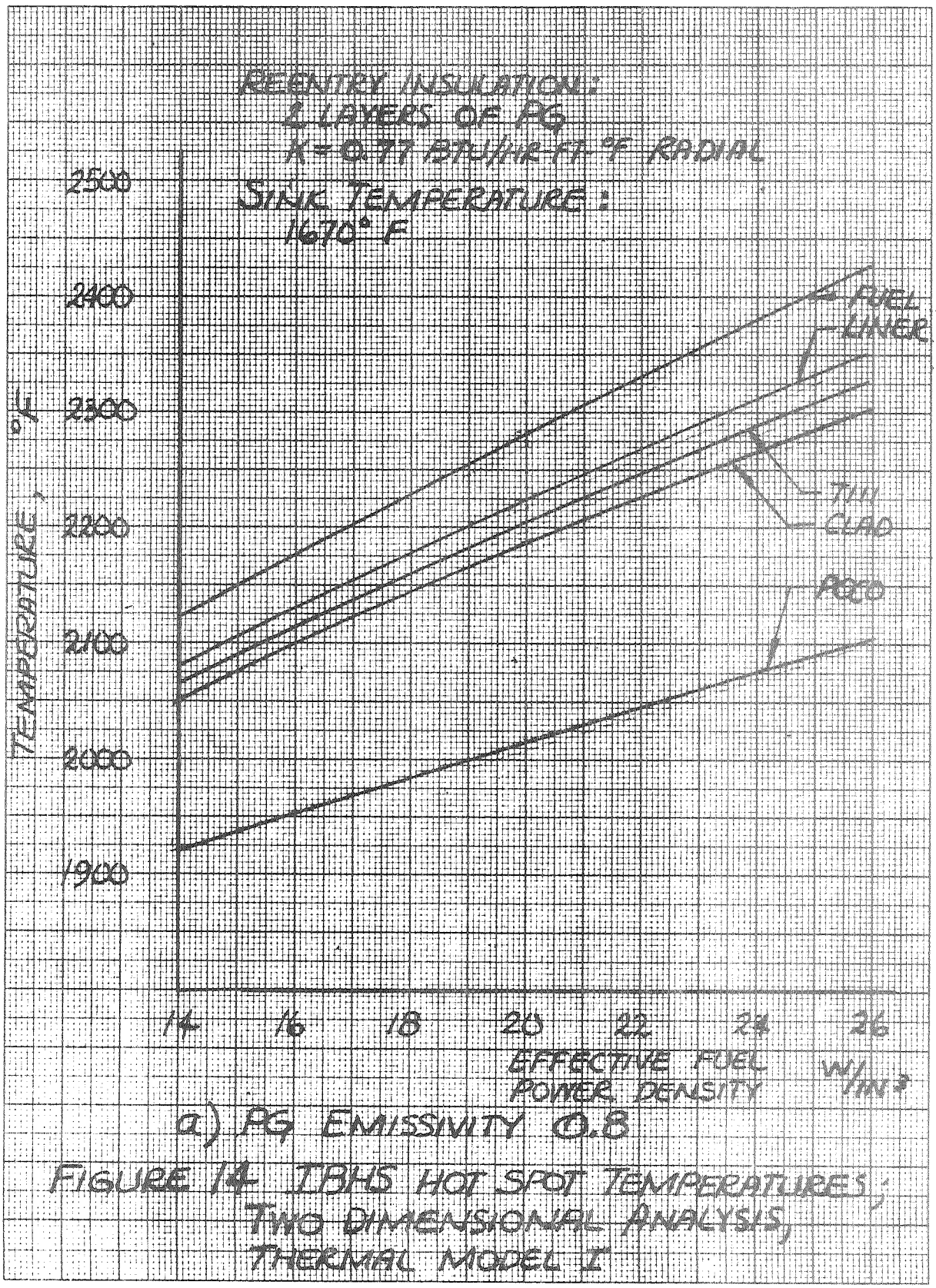

a) PG EMISSIVITY 0.8

FIGURE 14 TBHS HOT SPOT TEMPERATURES, TWO DIMENSIONAL ANALYSIS, THERMAL MODEL I

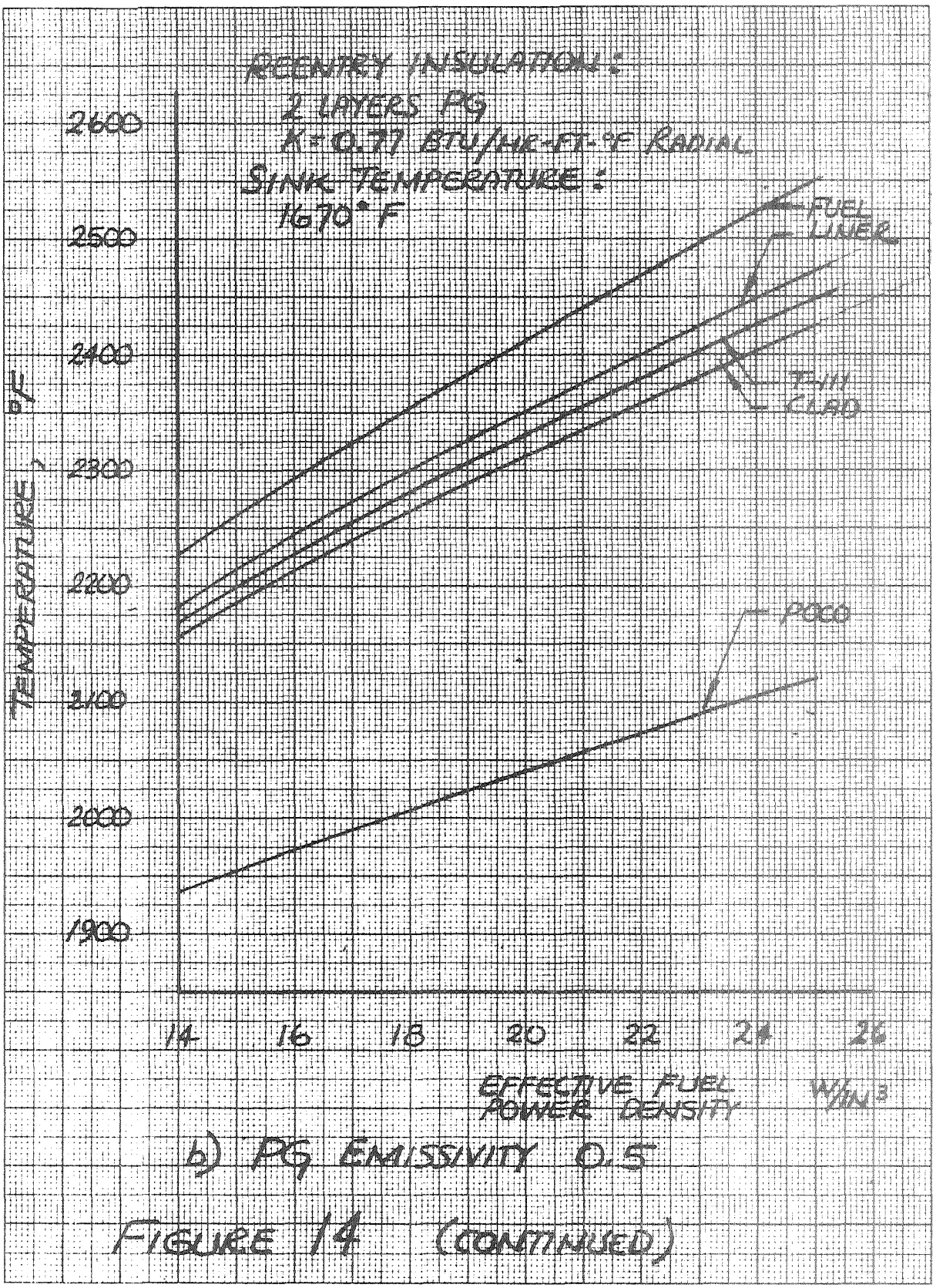

b) PG EMISSIVITY 0.5

FIGURE 14 (CONTINUED)

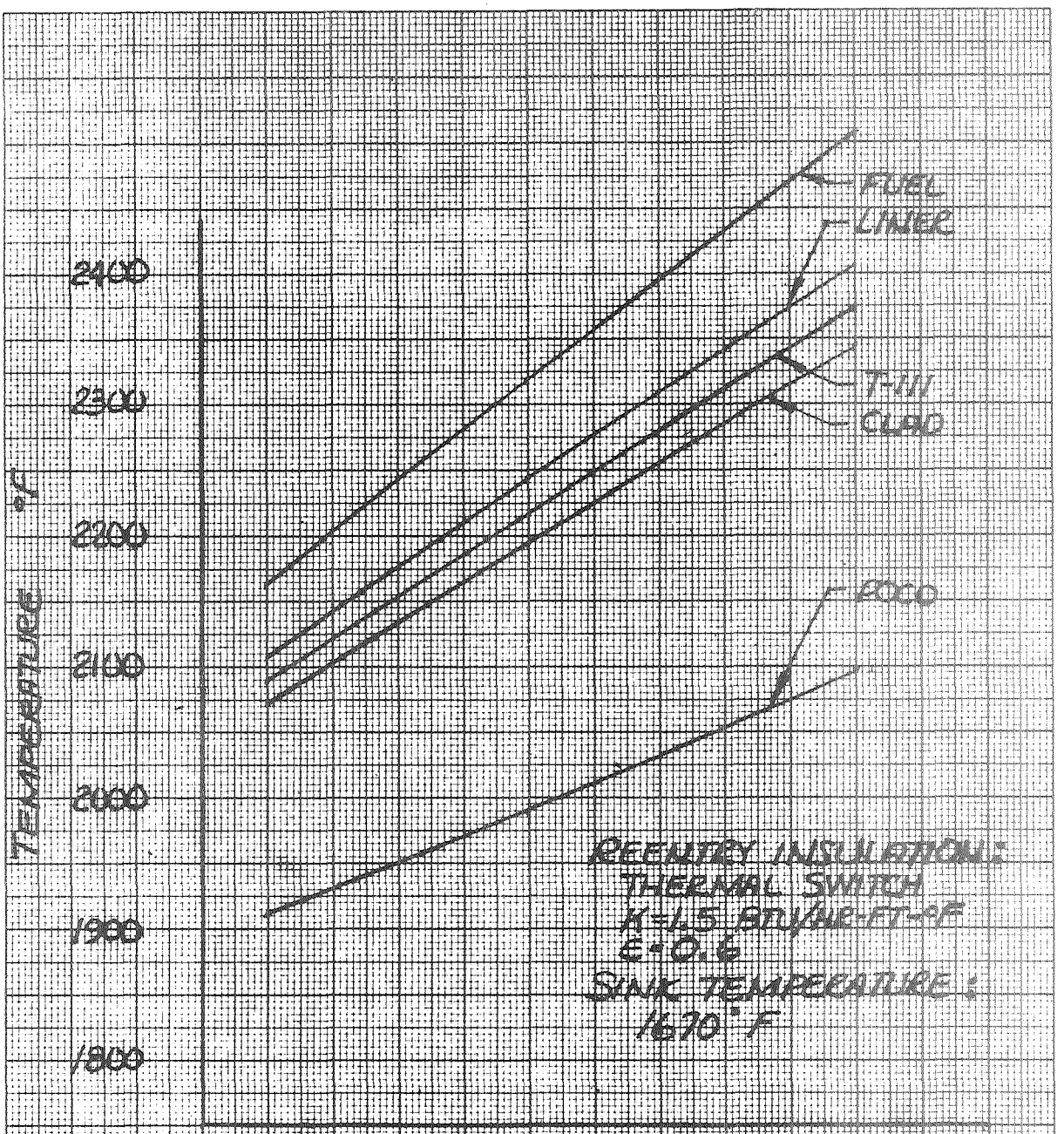

a) 6.3 INCH LONG CAPSULE

FIGURE 15 IBHS HOT SPOT TEMPERATURE, TWO DIMENSIONAL ANALYSIS, THERMAL MODEL II

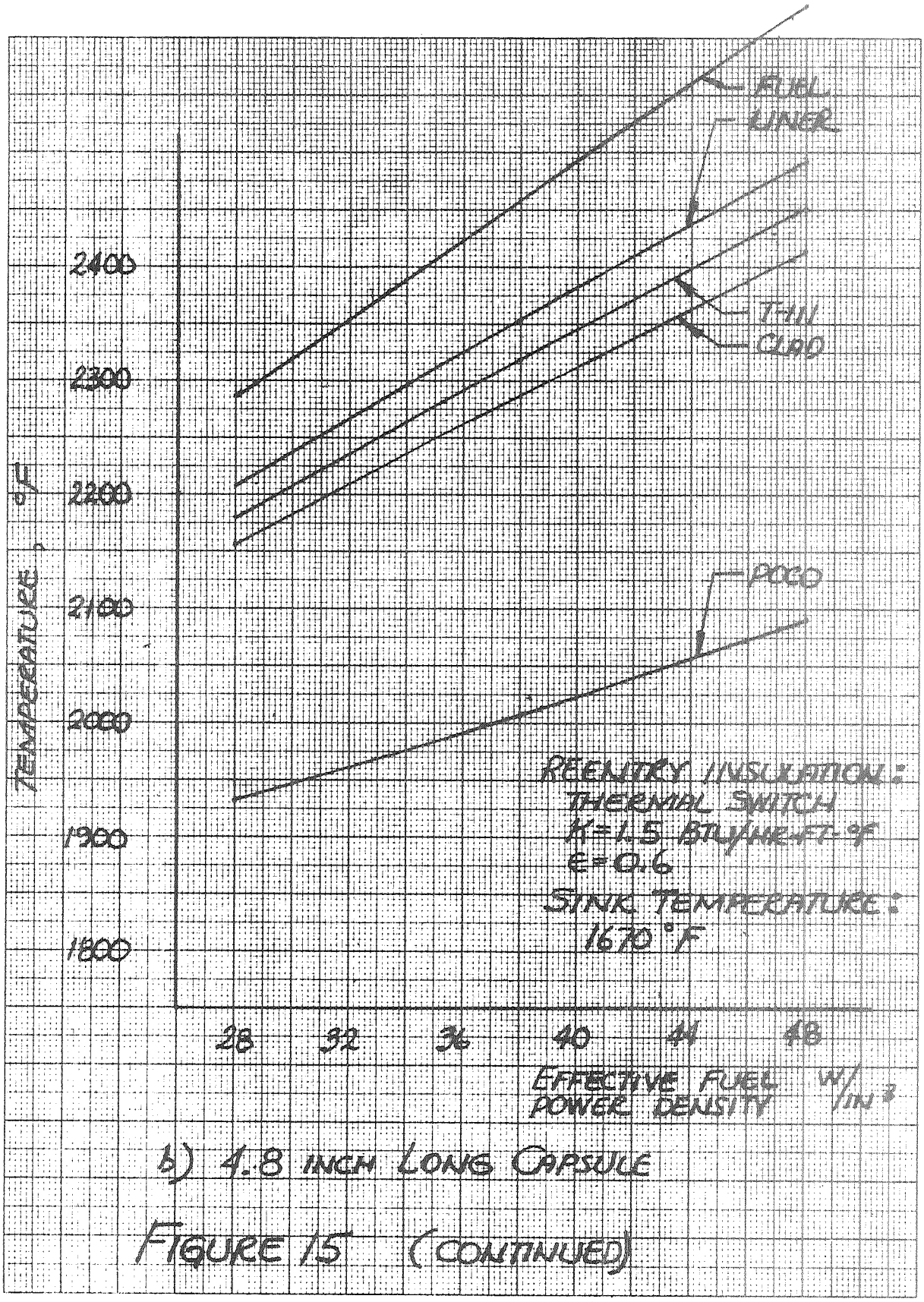

b) 4.8 INCH LONG CAPSULE

FIGURE 15 (CONTINUED)

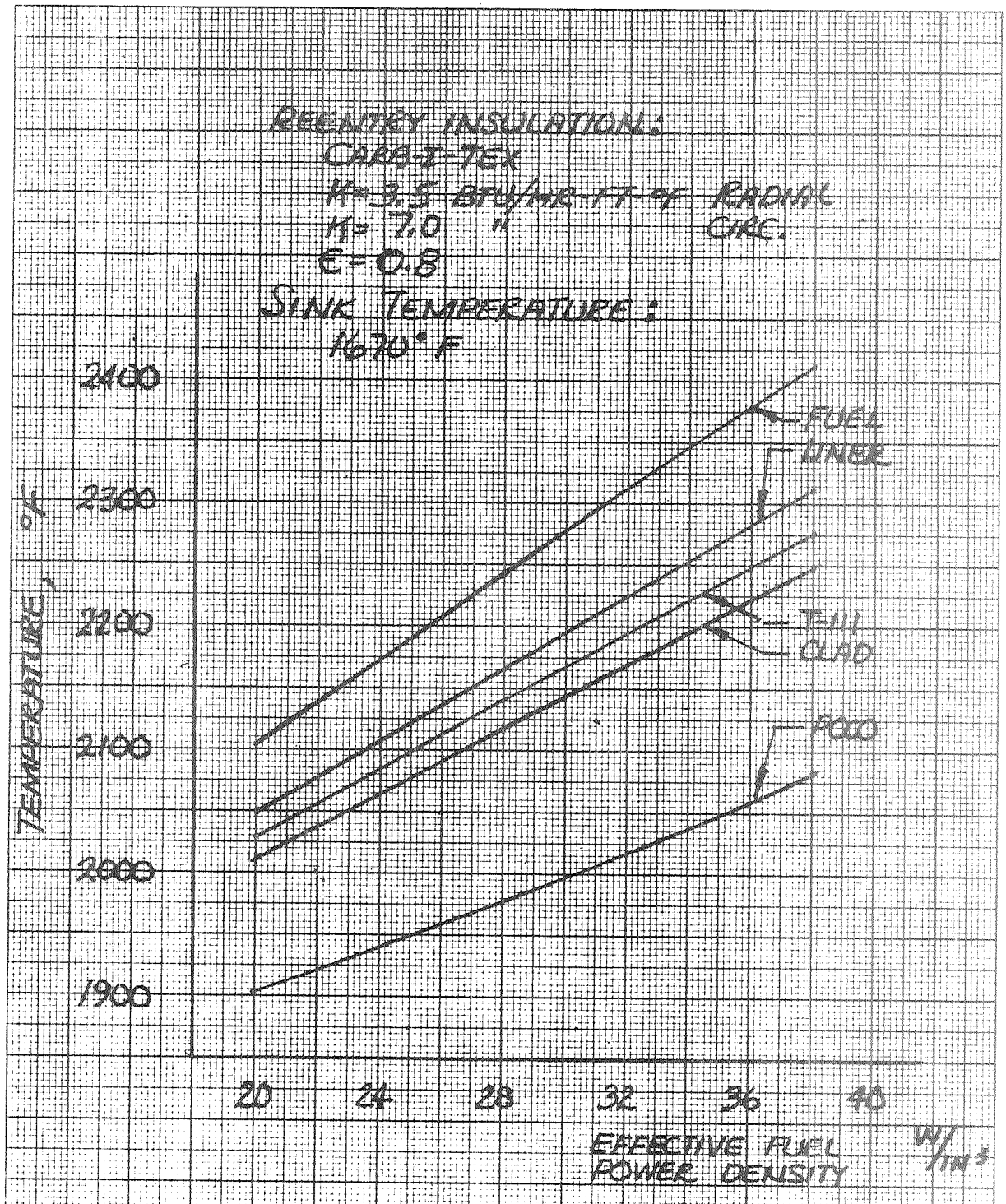

FIGURE 16 IBHS HOT SPOT TEMPERATURES, TWO DIMENSIONAL ANALYSIS, THERMAL MODEL II 6.3 INCH LONG CAPSULE

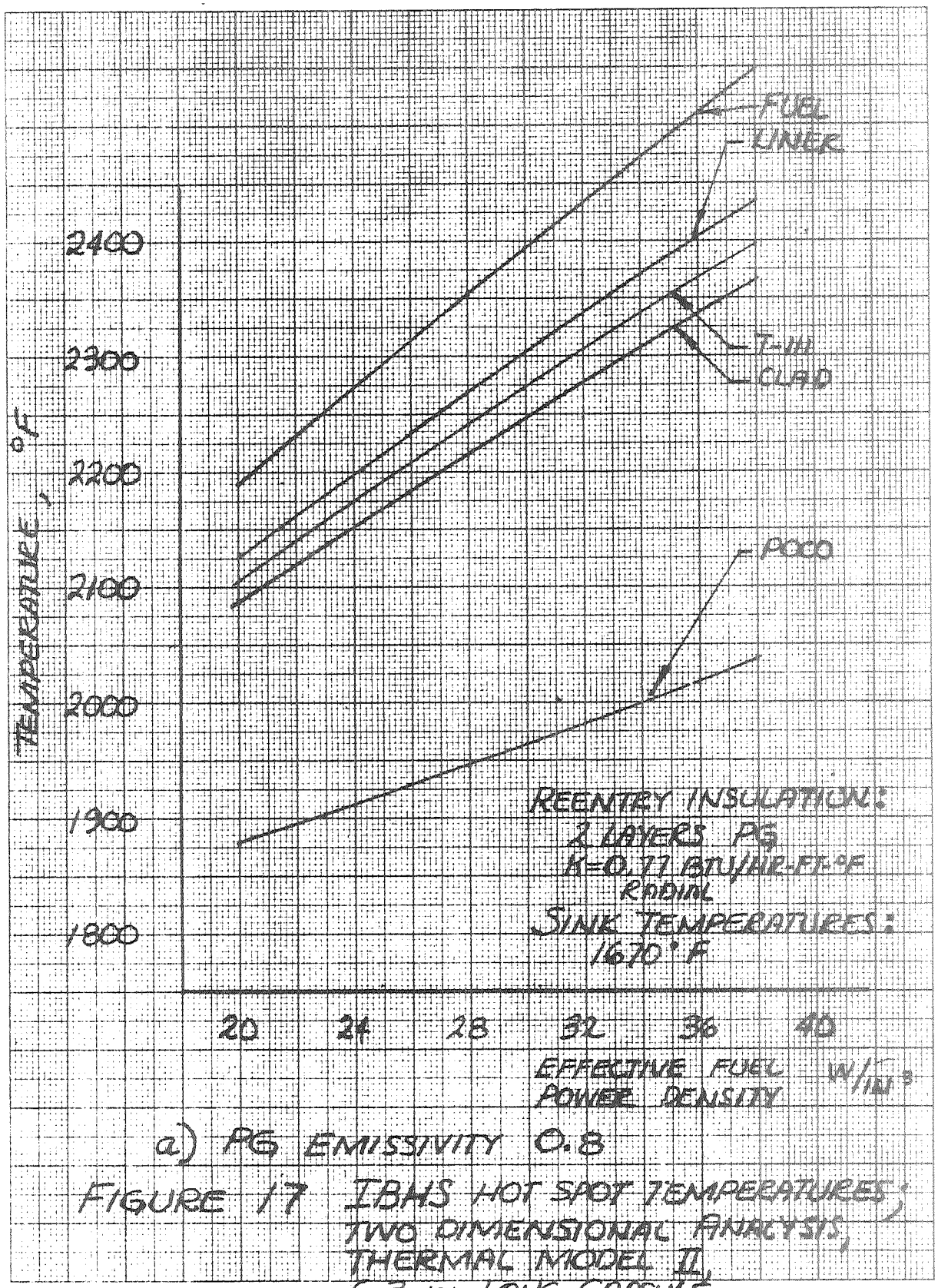

a) PG EMISSIVITY 0.8

FIGURE 17 IBHS HOT SPOT TEMPERATURES, TWO DIMENSIONAL ANALYSIS, THERMAL MODEL II, 6.3 IN LONG CAPSULE

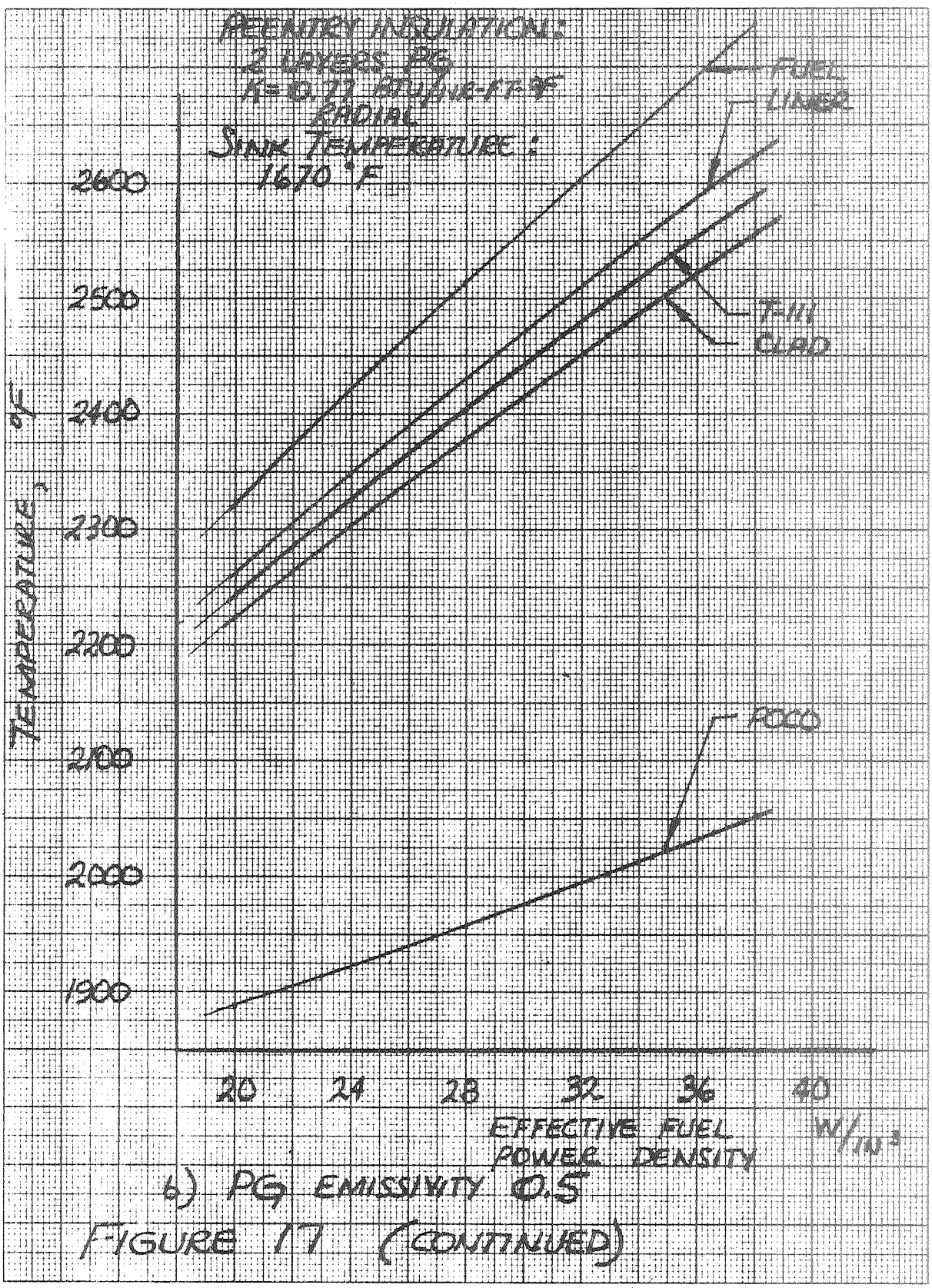

b) PG EMISSIVITY 0.5

FIGURE 17 (CONTINUED)

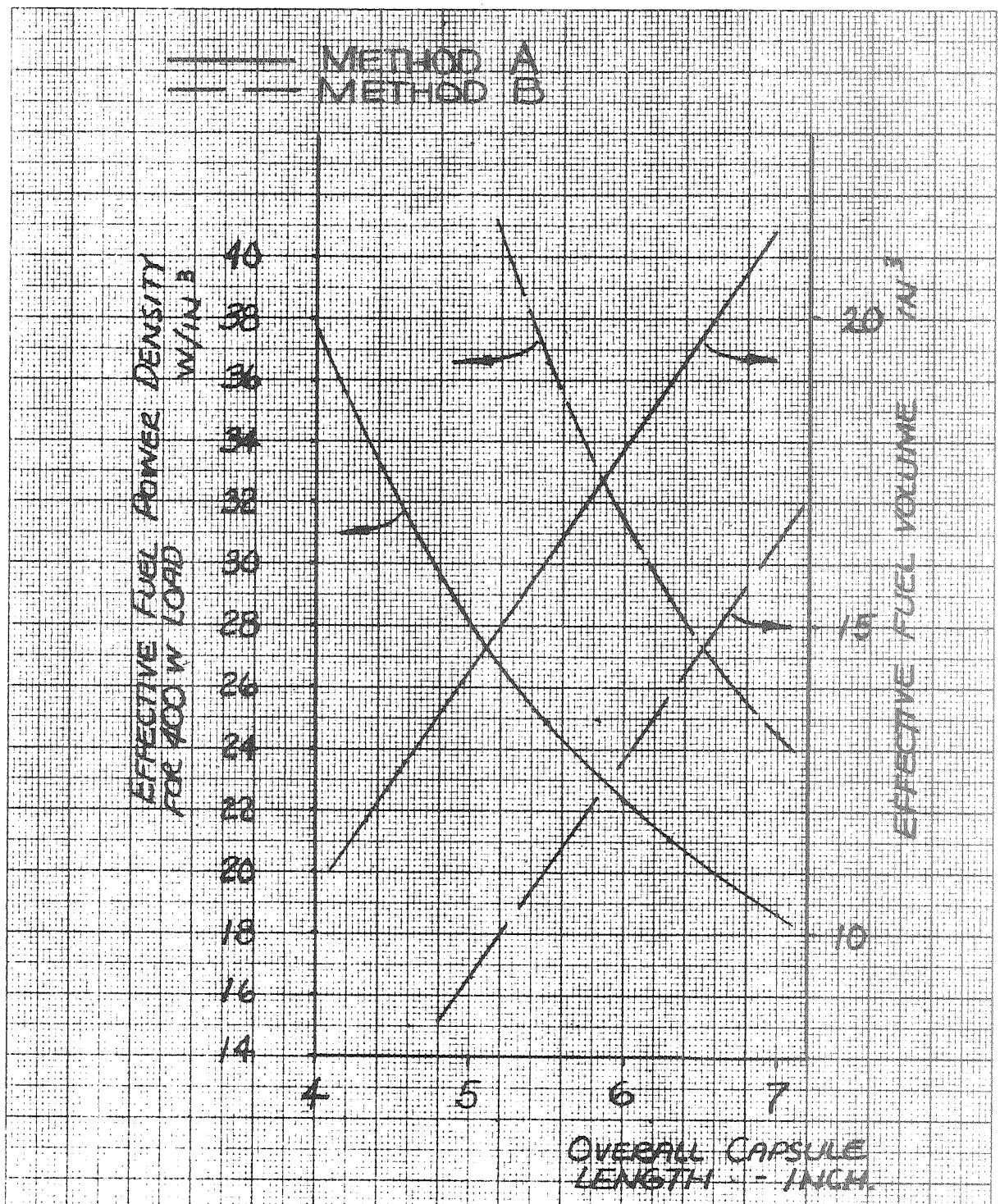

FIGURE 18 ESTIMATES OF EFFECTIVE FUEL VOLUME AND EFFECTIVE POWER DENSITY FOR IEHS TWO DIMENSIONAL ANALYSIS

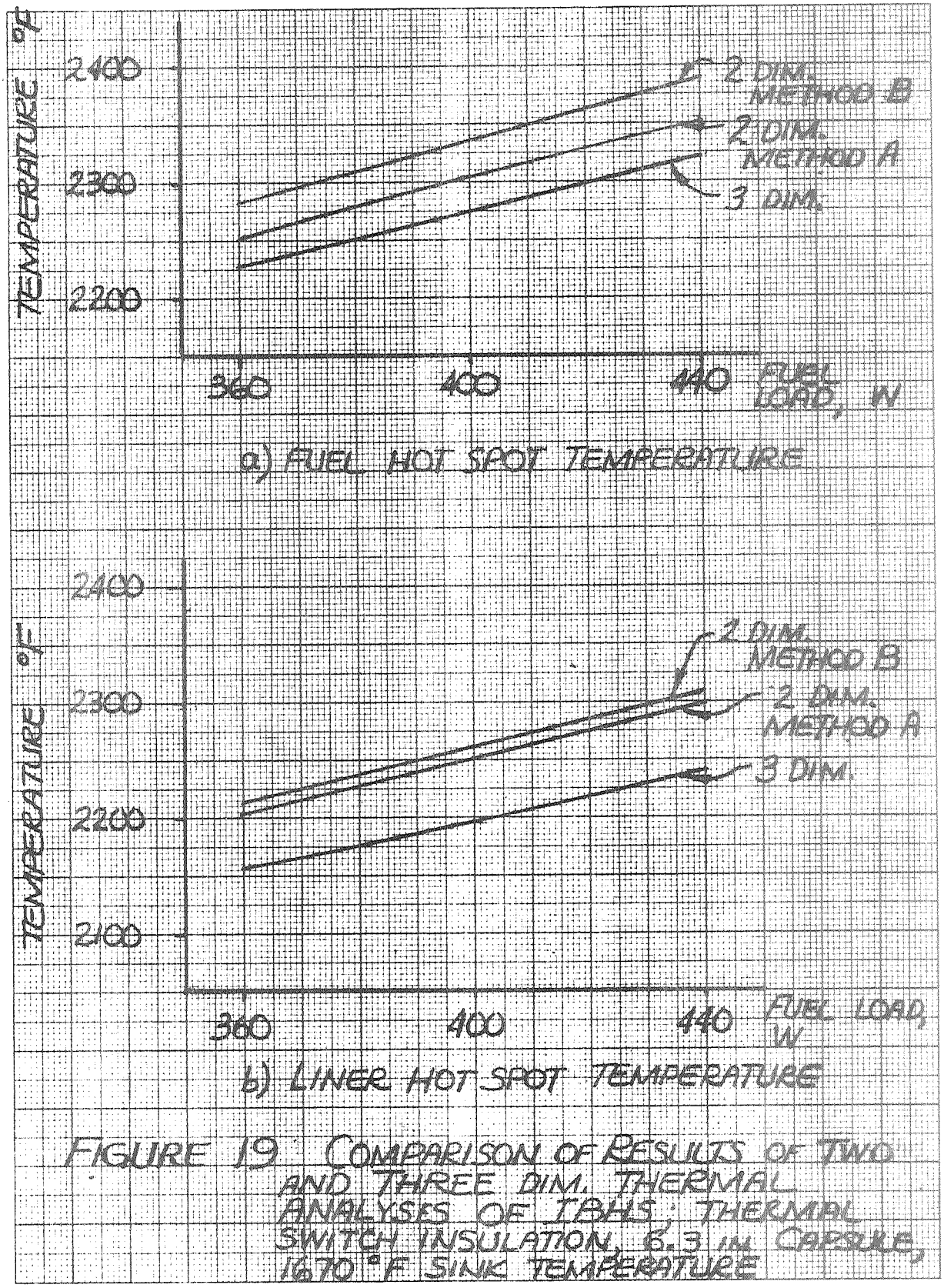

FIGURE 19 COMPARISON OF RESULTS OF TWO AND THREE DIM. THERMAL ANALYSES OF TBHS: THERMAL SWITCH INSULATION, 6.3 IN. CAPSULE, 1670 °F SINK TEMPERATURE

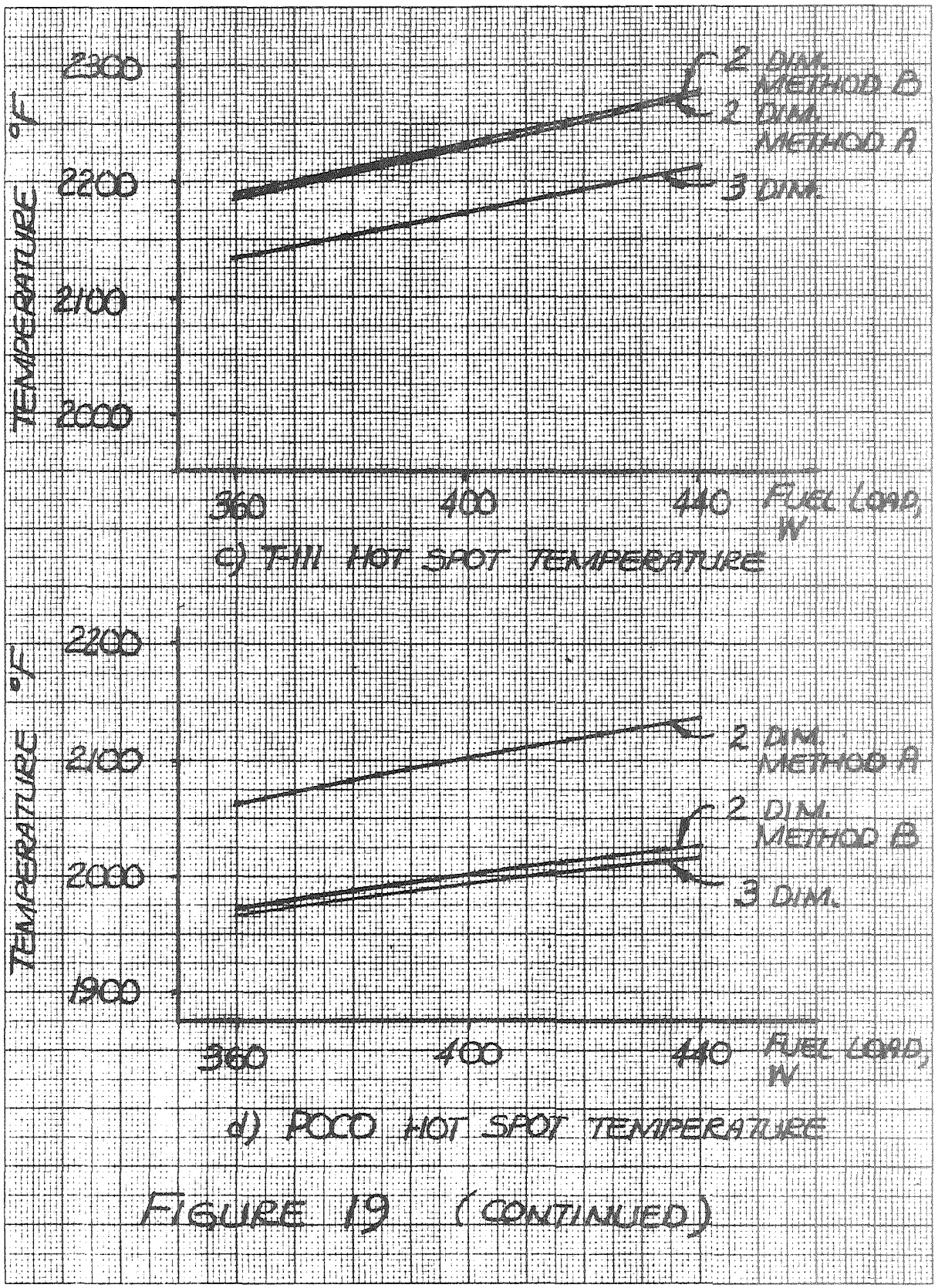

FIGURE 19 (CONTINUED)

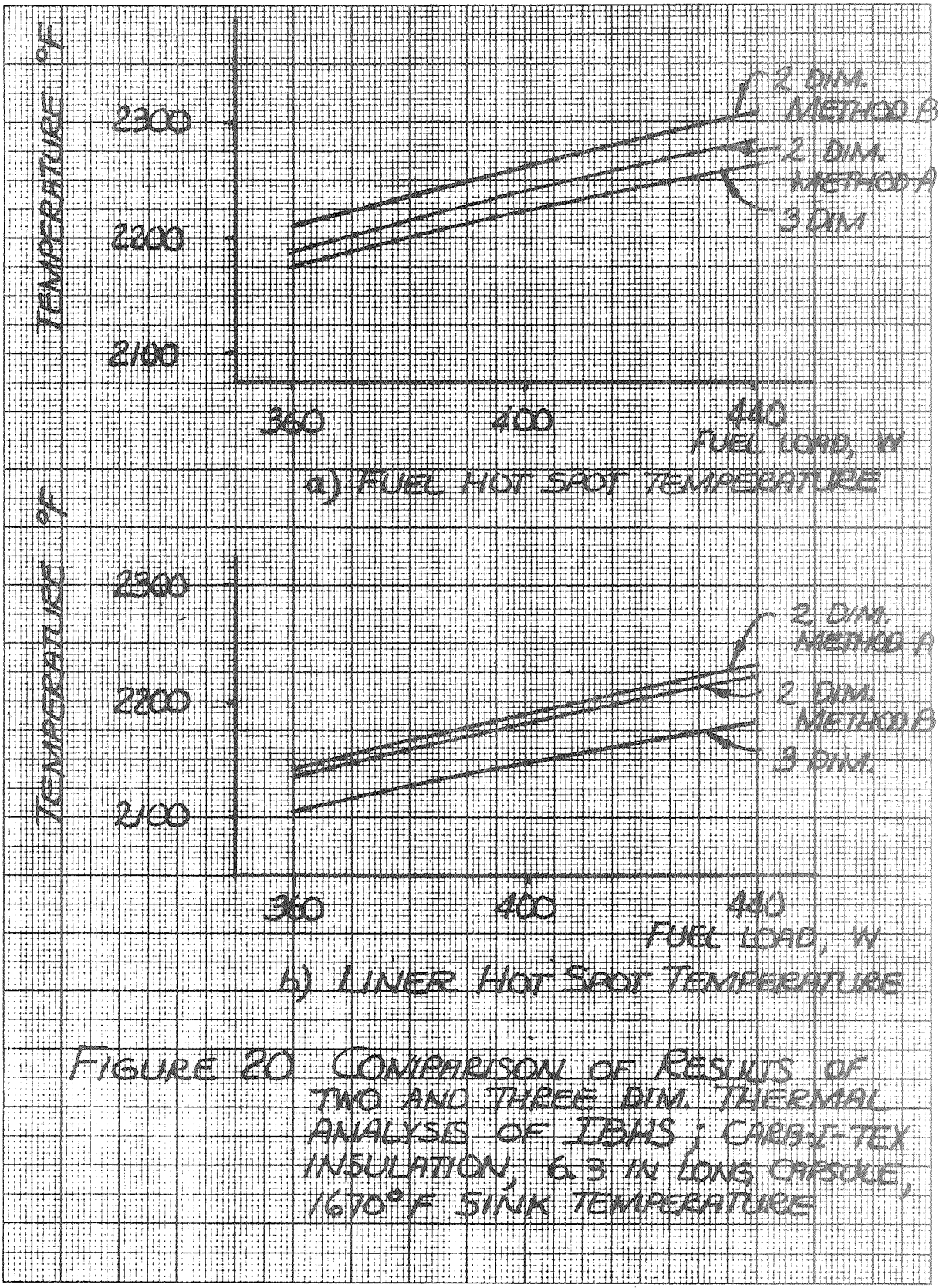

FIGURE 20 COMPARISON OF RESULTS OF TWO AND THREE DIM. THERMAL ANALYSES OF IBHS; CARB-I-TEX INSULATION, 6.3 IN LONG CAPSULE, 1670° F SINK TEMPERATURE

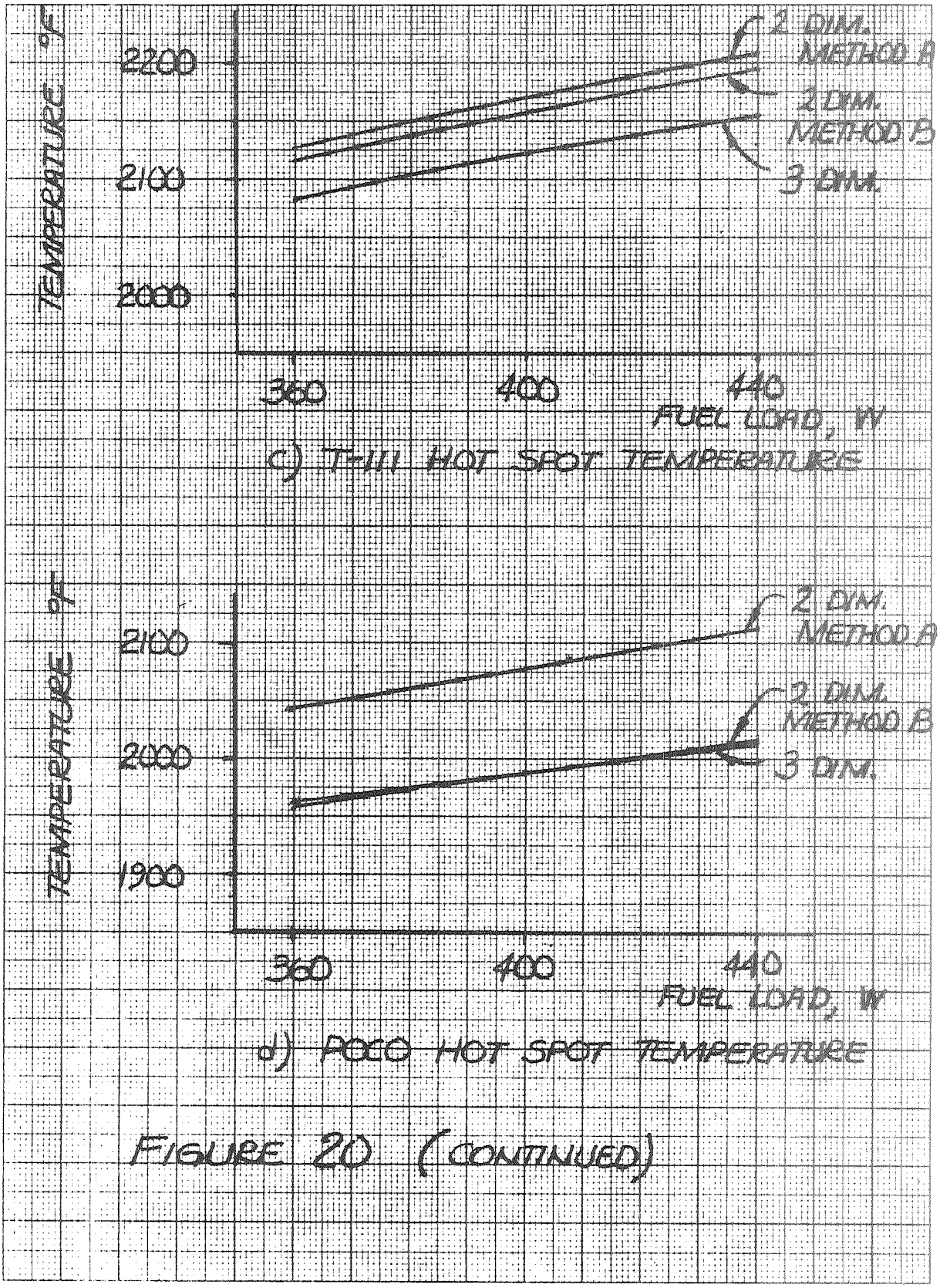

FIGURE 20 (CONTINUED)

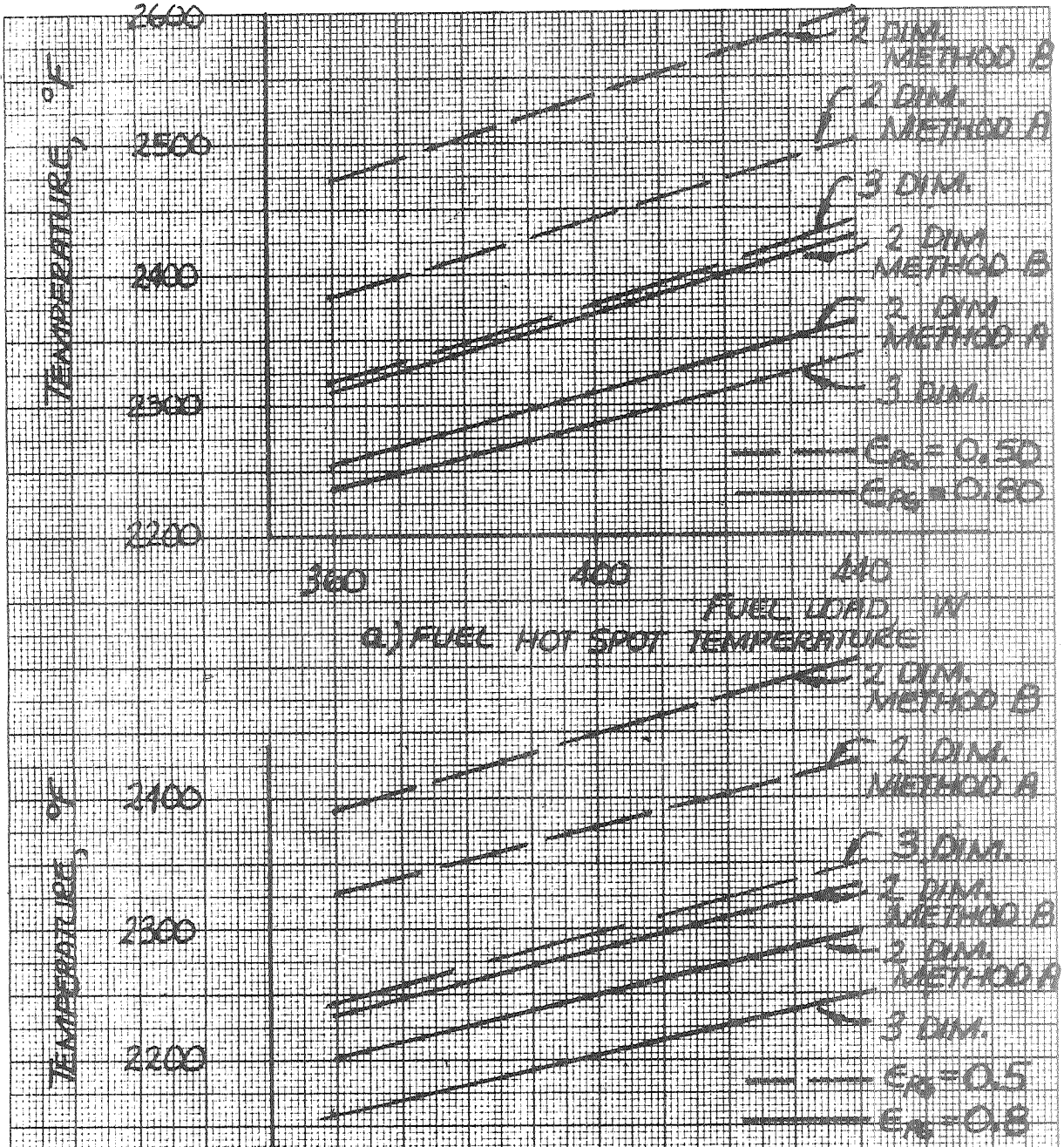

FIGURE 21 COMPARISON OF RESULTS OF TWO AND THREE DIM. THERMAL ANALYSIS OF TEHS | 2 LAYERS OF P_S INSULATION, 6.3 IN LONG CAPSULE, 1610° F SINK TEMPERATURE.

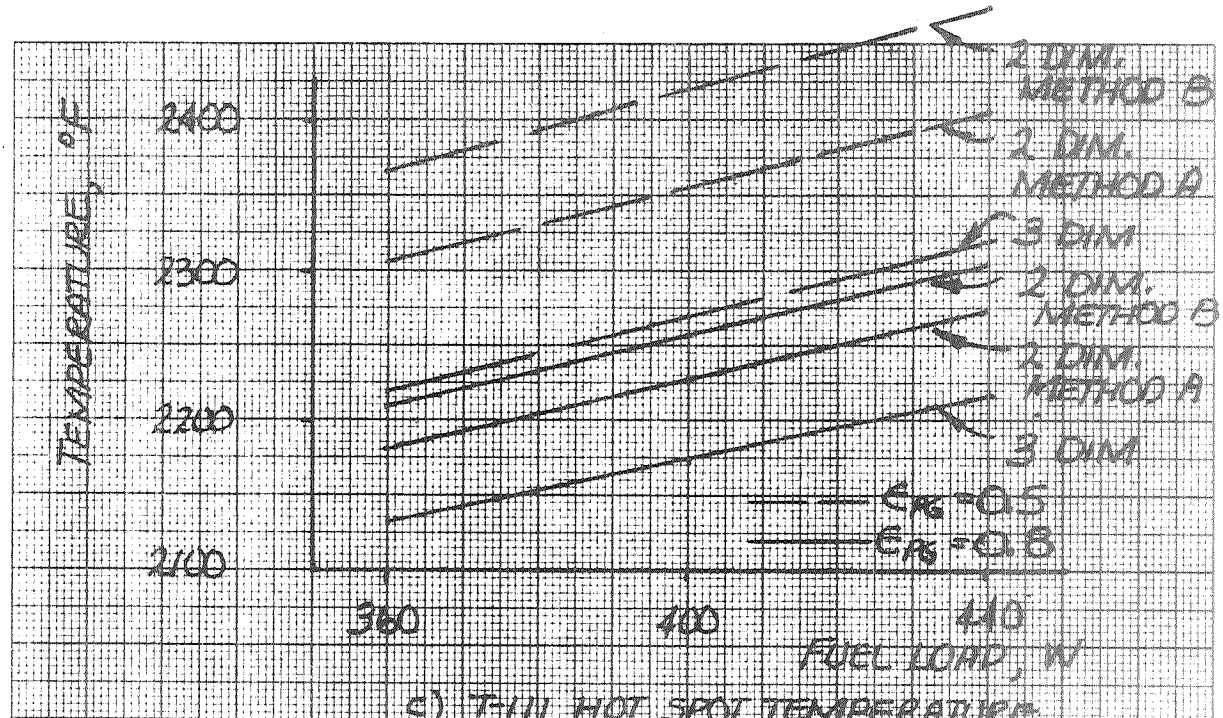

c) T-111 HOT SPOT TEMPERATURE

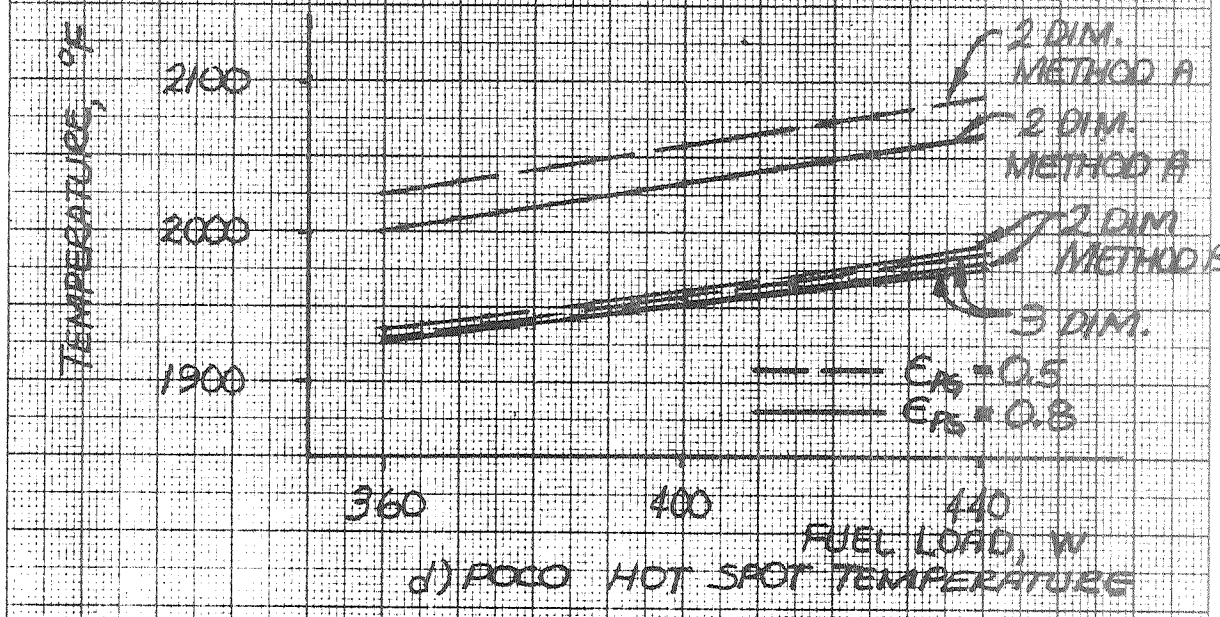

d) POCO HOT SPOT TEMPERATURE

FIGURE 21 (CONTINUED)

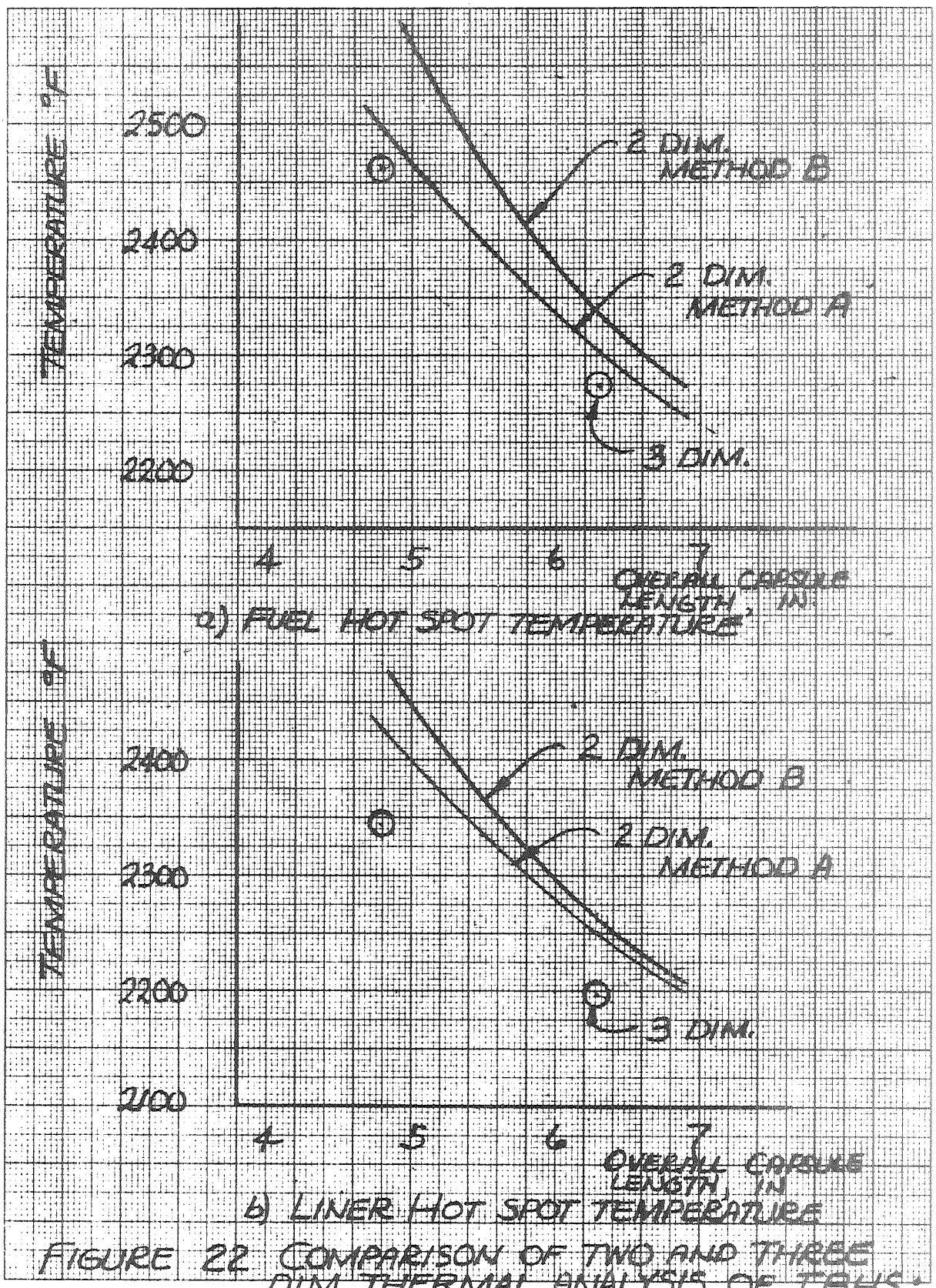

FIGURE 22 COMPARISON OF TWO AND THREE DIM THERMAL ANALYSIS OF IBHS, THERMAL SWITCH INSULATION, 400 W FUEL LOAD, 1670° F SINK TEMPERATURE.

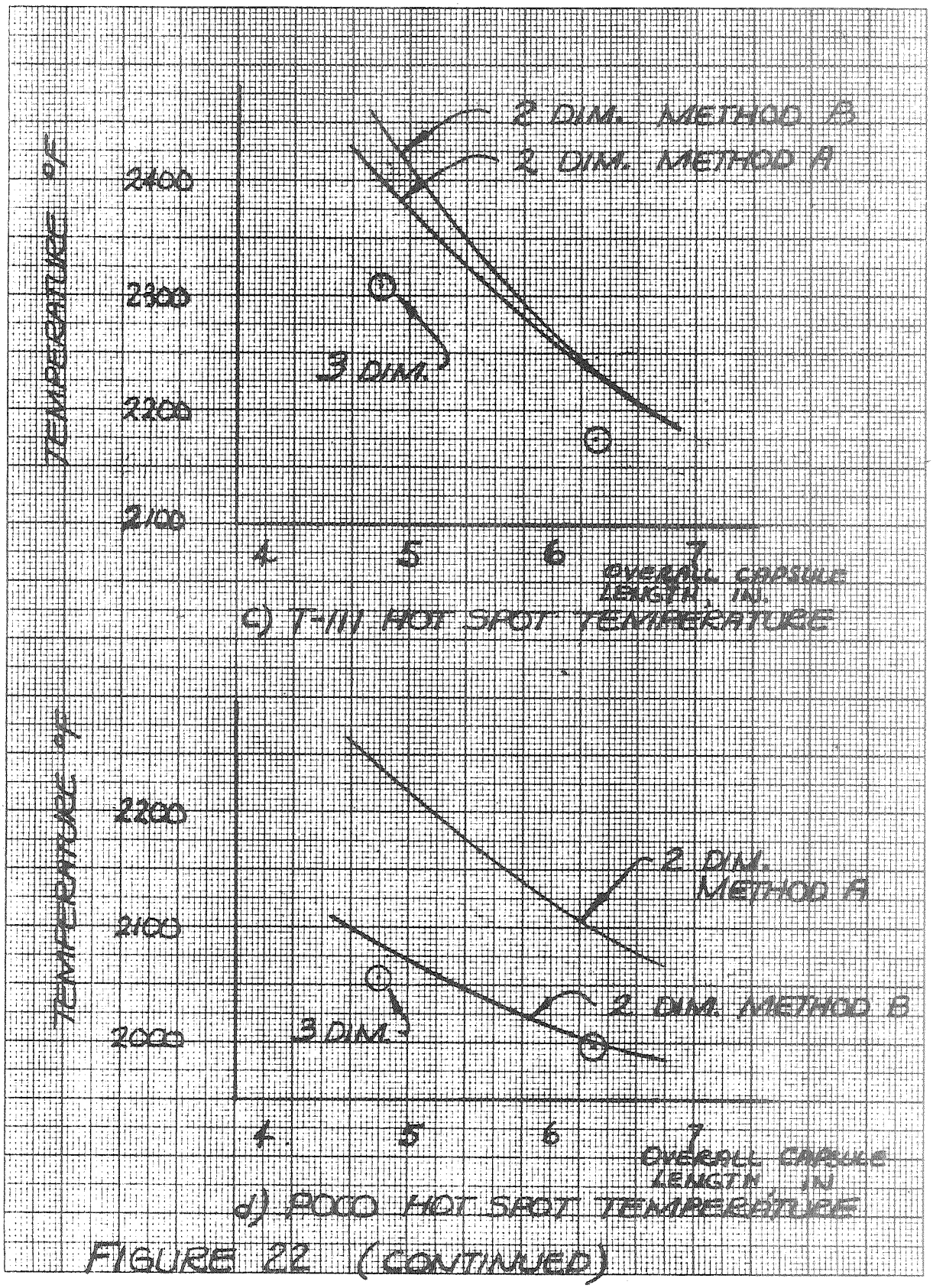

FIGURE 22 (CONTINUED)

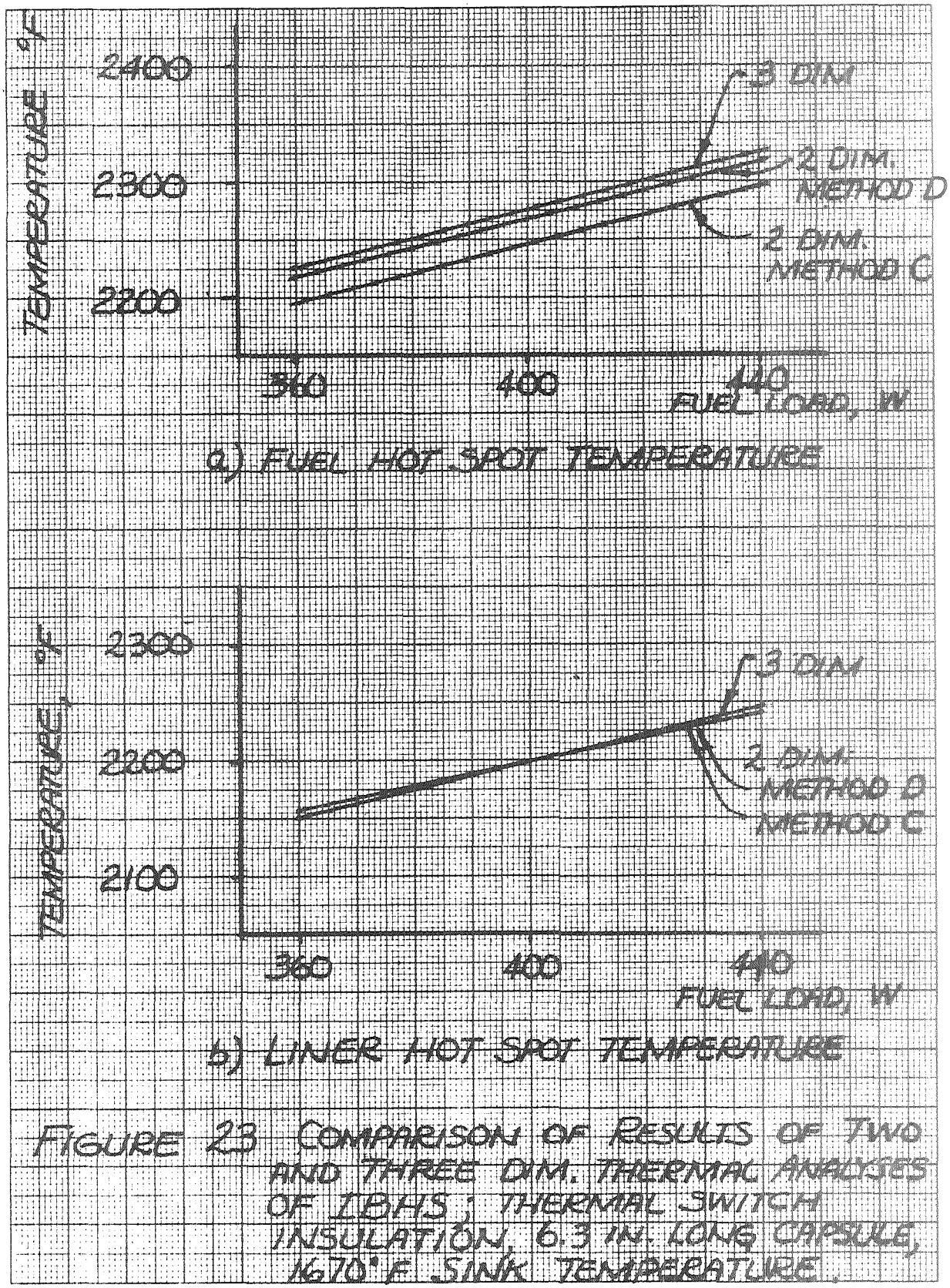

FIGURE 23 COMPARISON OF RESULTS OF TWO AND THREE DIM. THERMAL ANALYSES OF IBHS; THERMAL SWITCH INSULATION, 6.3 IN. LONG CAPSULE, 70°F SINK TEMPERATURE.

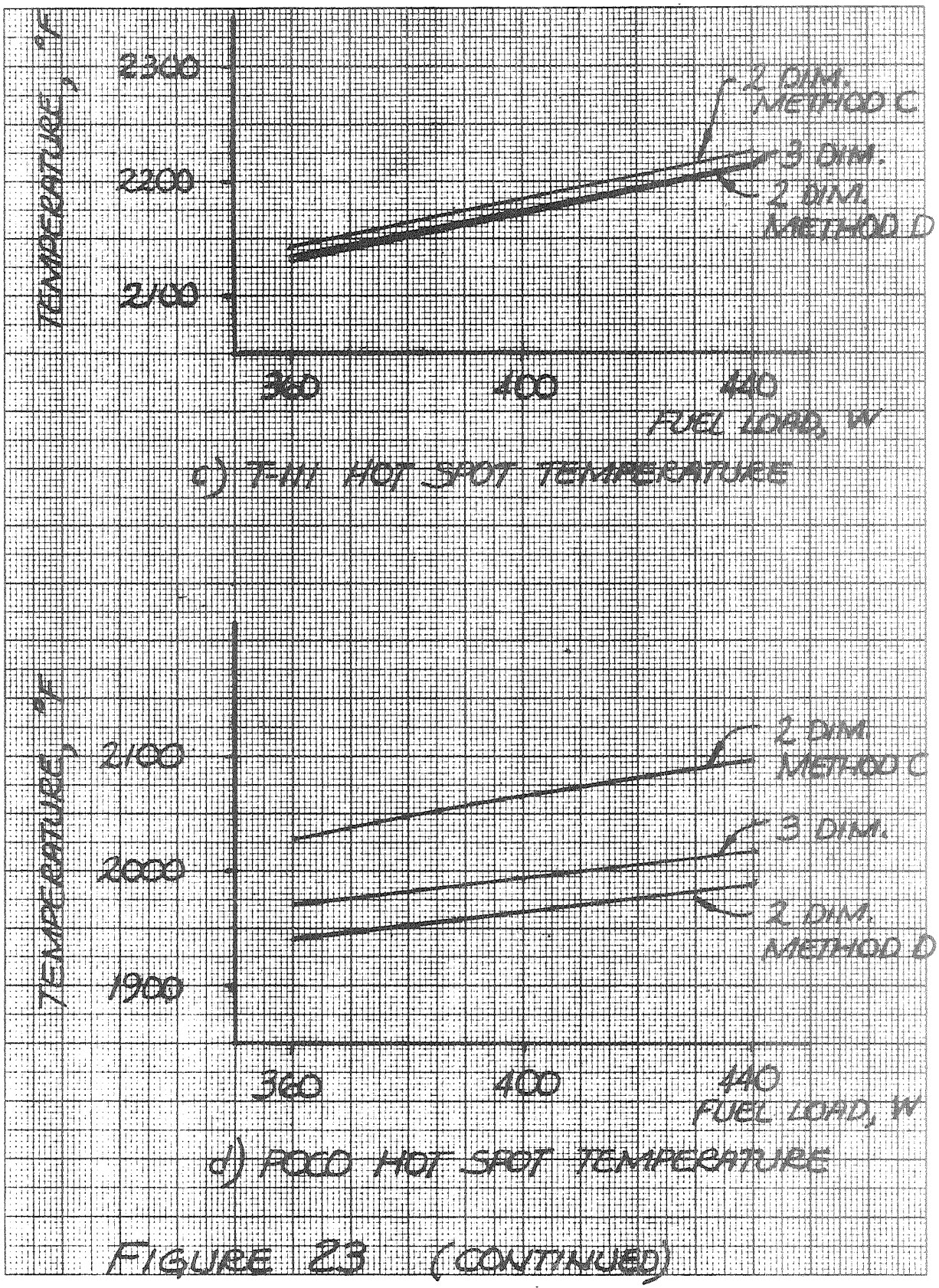

FIGURE 23 (CONTINUED)

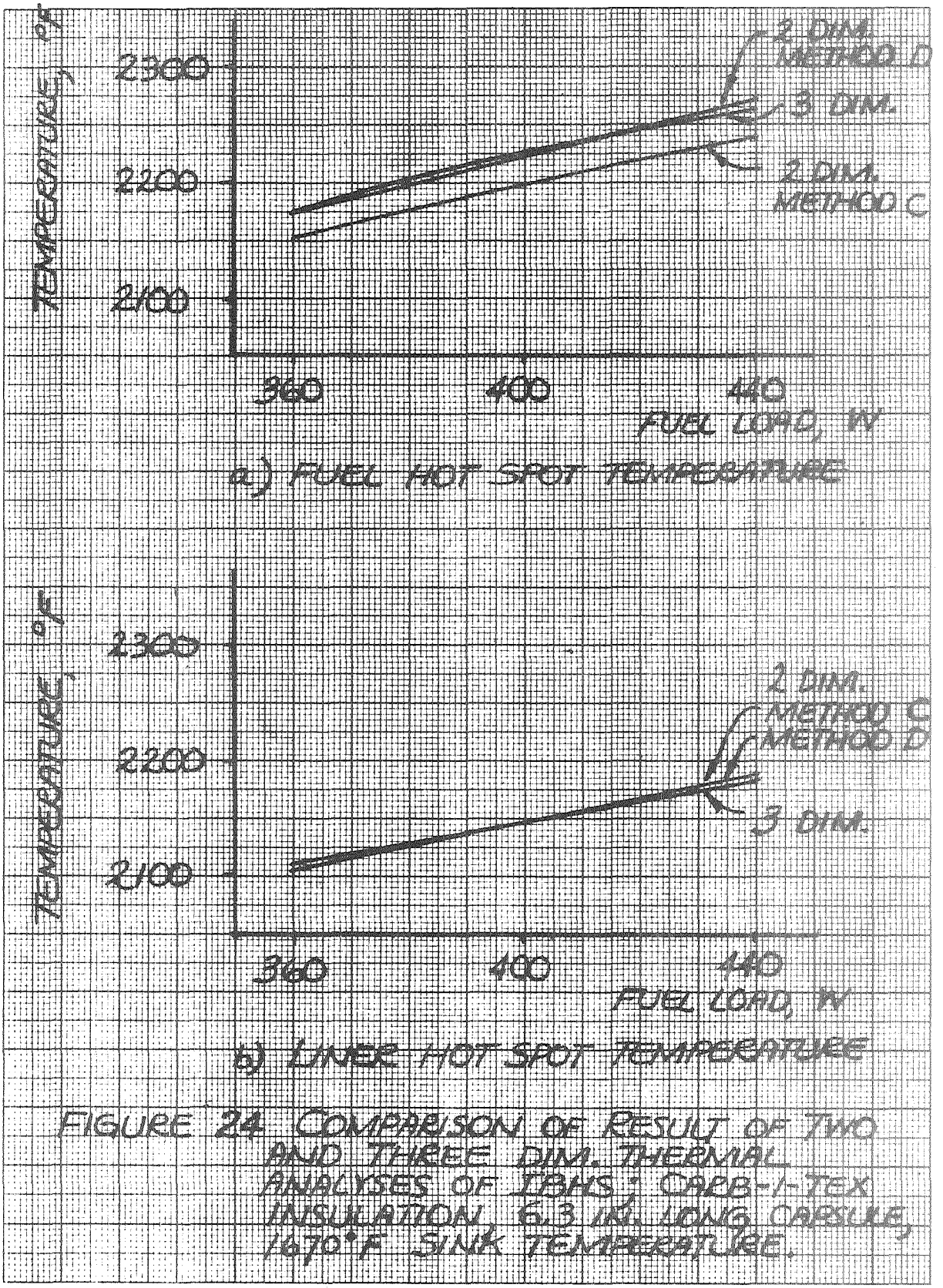

FIGURE 24 COMPARISON OF RESULT OF TWO AND THREE DIM. THERMAL ANALYSES OF IBHS ; CARB-I-TEX INSULATION, 6.3 IN. LONG CAPSULE, 1670°F SINK TEMPERATURE.

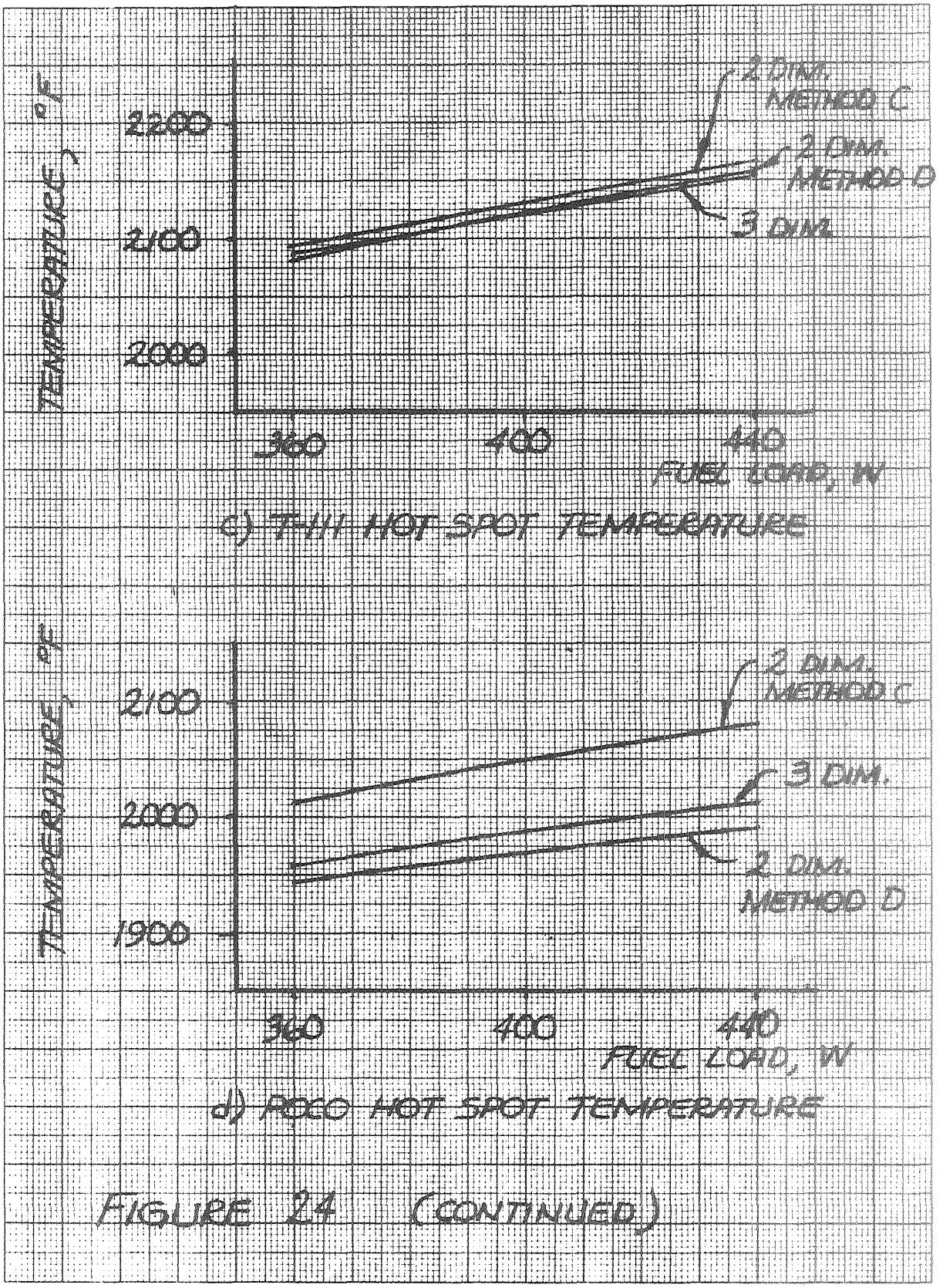

FIGURE 24 (CONTINUED)

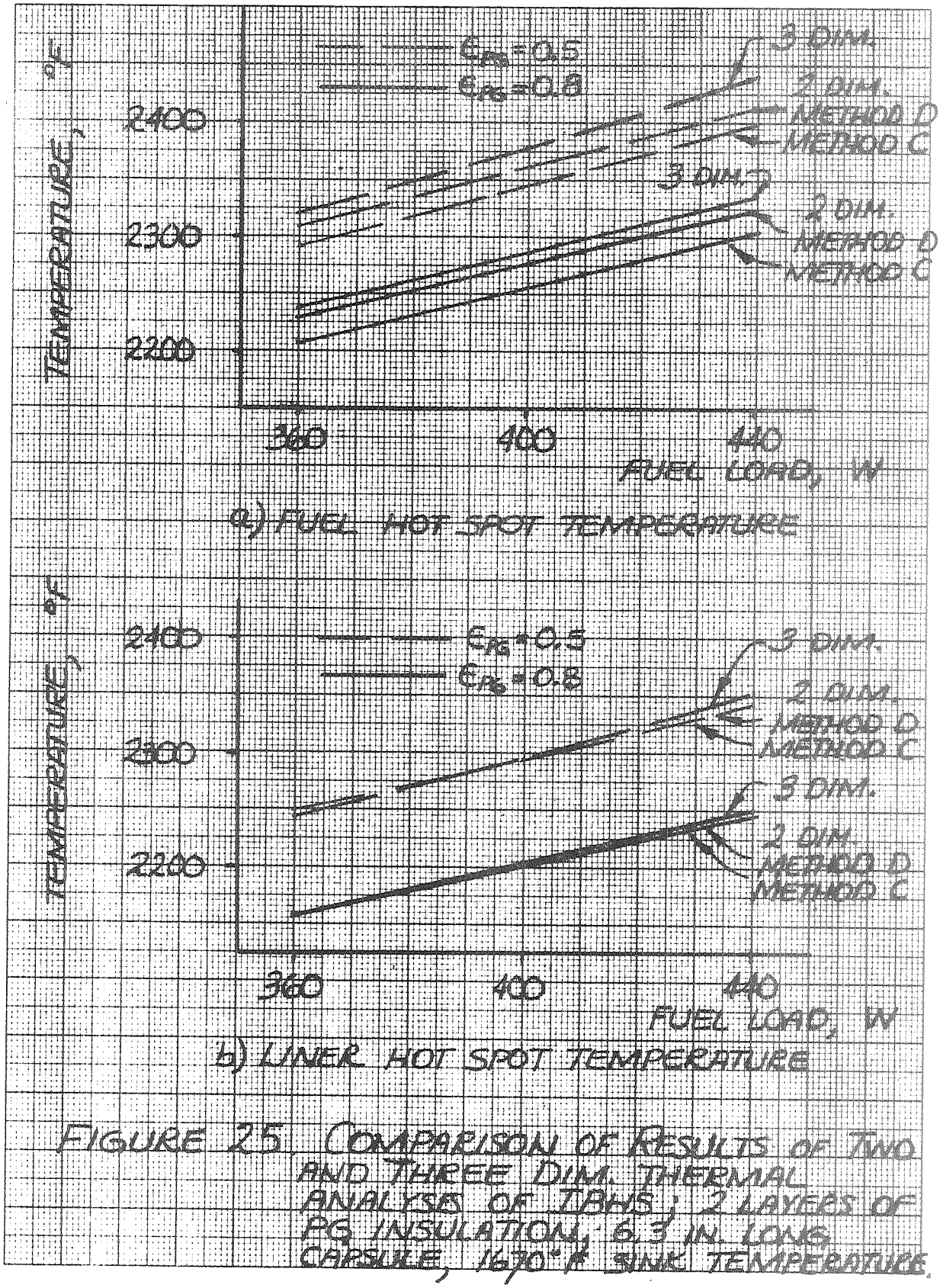

FIGURE 25. COMPARISON OF RESULTS OF TWO AND THREE DIM. THERMAL ANALYSES OF TBHS; 2 LAYERS OF PG INSULATION, 6.3" IN. LONG CAPSULE, 1670°F SINK TEMPERATURE.

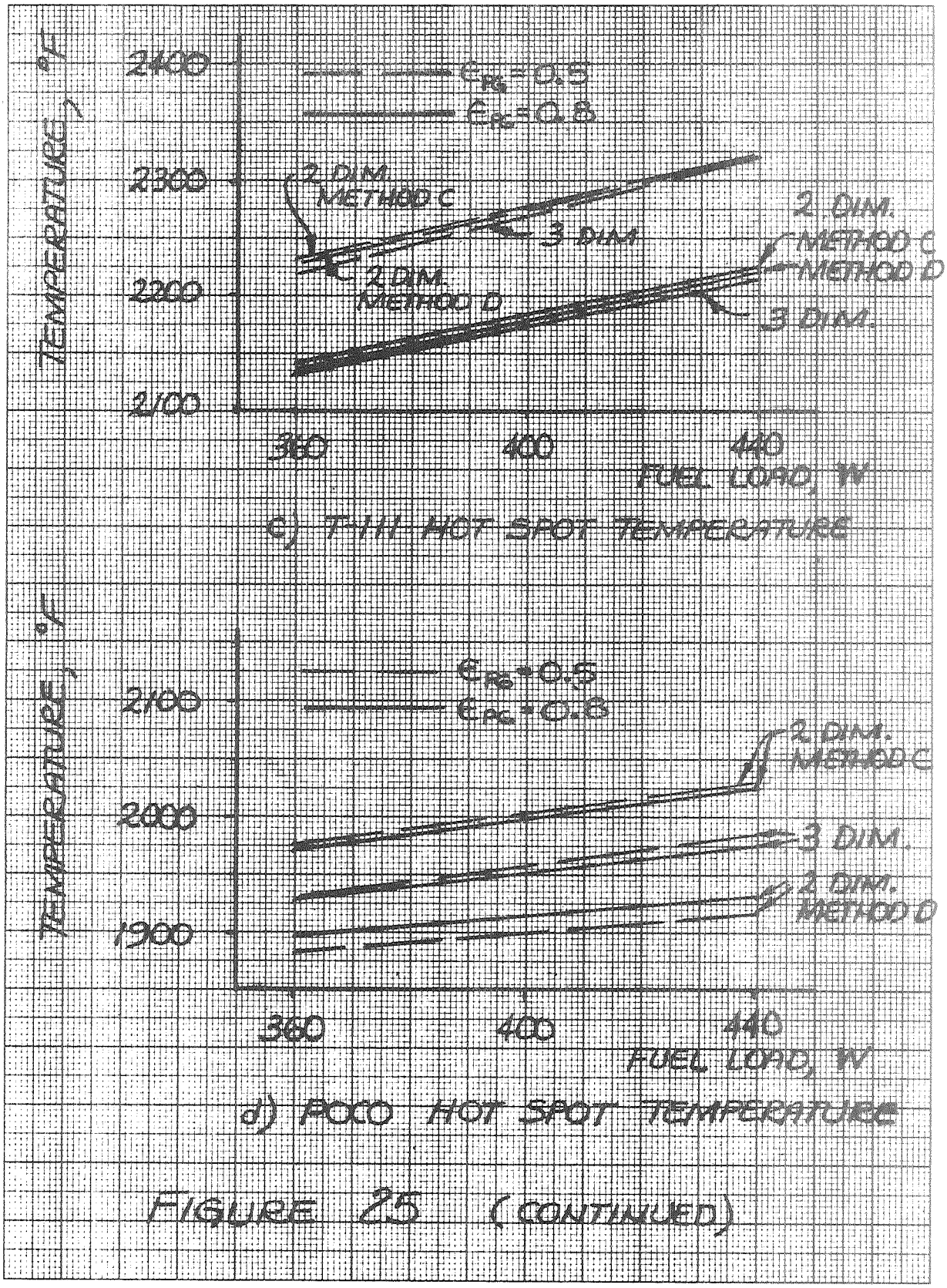

FIGURE 25 (CONTINUED)

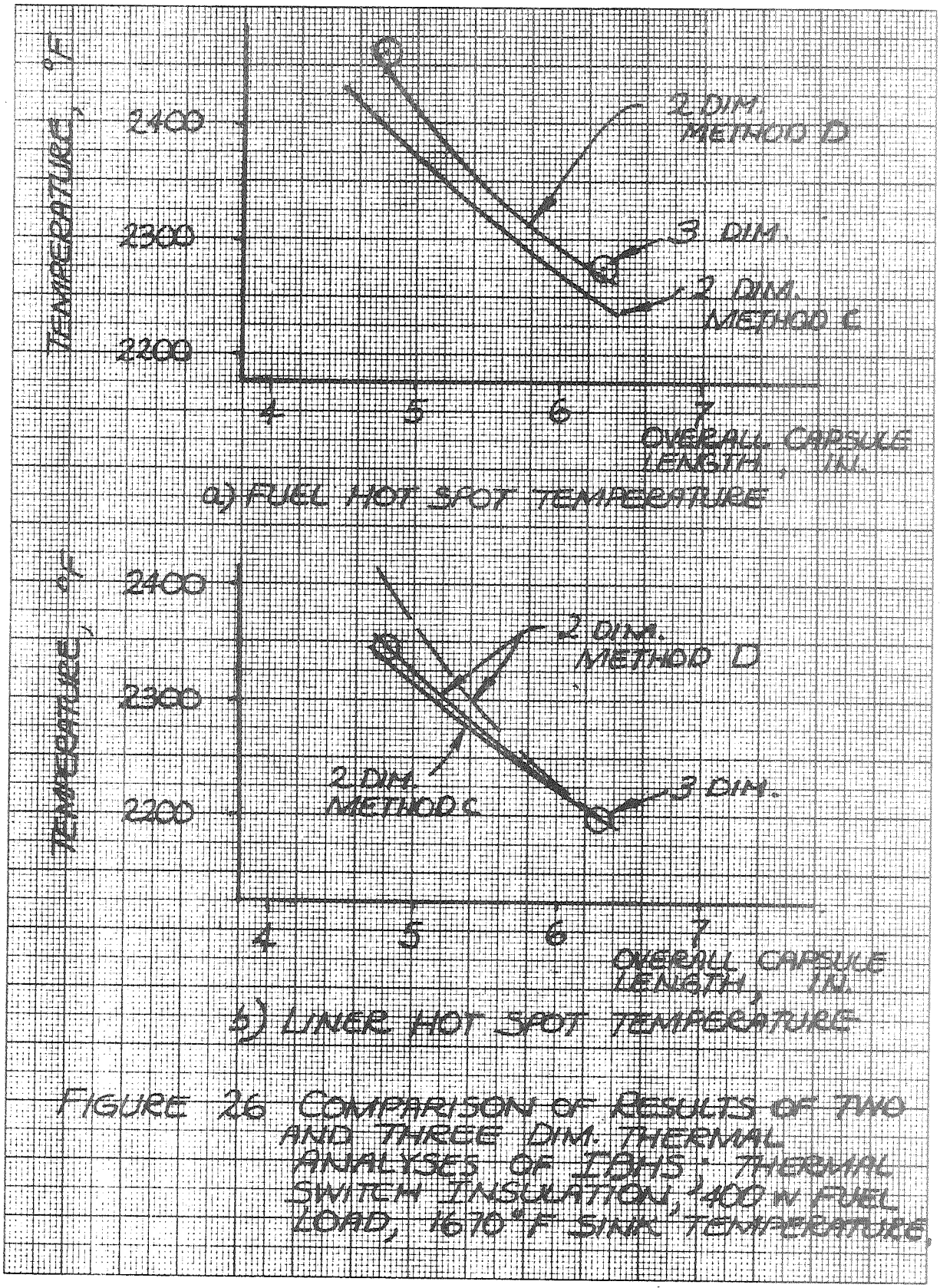

FIGURE 26 COMPARISON OF RESULTS OF TWO AND THREE DIM. THERMAL ANALYSES OF EBHS: THERMAL SWITCH INSULATION, 400 W FUEL LOAD, 1610°F SINK TEMPERATURE,

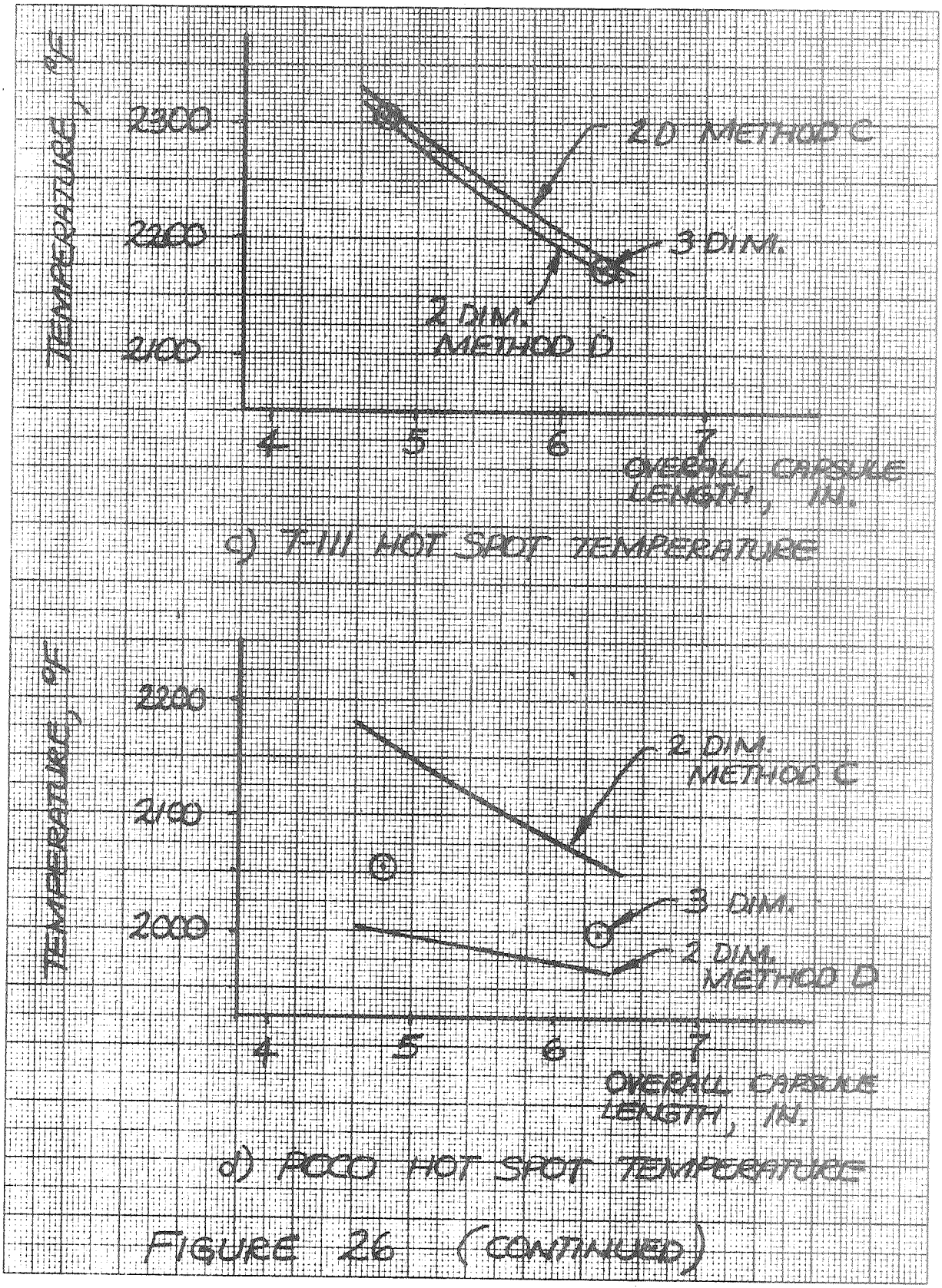

FIGURE 26 (CONTINUED)